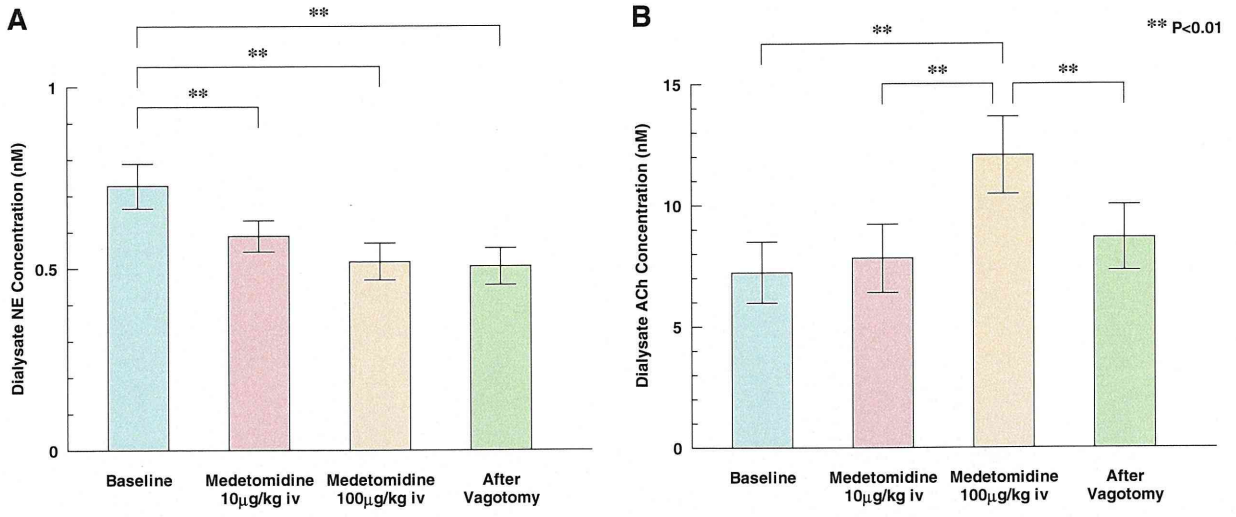

Figure 2. Effects of intravenous administration of low and high doses of medetomidine on dialysate NE (**A**) and ACh concentrations (**B**). Medetomidine at 10 and 100 μg/kg similarly decreased dialysate NE concentration (**A**). Medetomidine at 100 μg/kg significantly increased dialysate ACh concentration, but 10 μg/kg had no effect (**B**). Vagotomy suppressed the increase in dialysate ACh concentration. **P<0.01. ACh, acetylcholine; NE, norepinephrine.

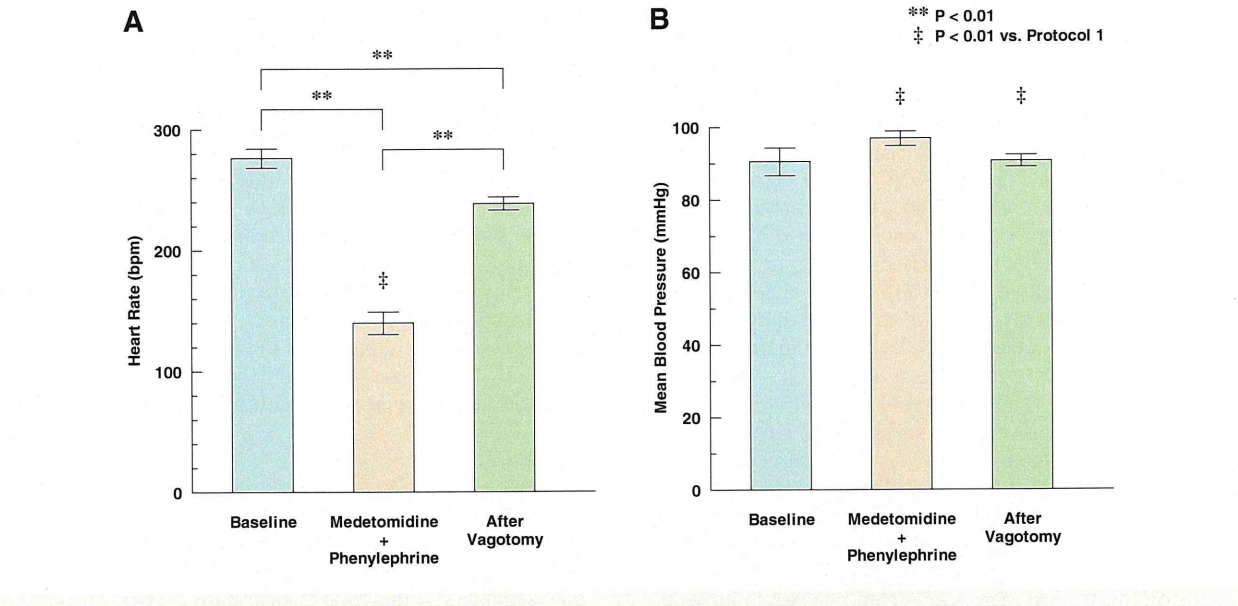

Figure 3. Effects of simultaneous intravenous administration of medetomidine and phenylephrine on heart rate (**A**) and mean blood pressure (**B**). Medetomidine combined with phenylephrine significantly decreased heart rate (**A**), and the decrease was significantly greater compared with medetomidine alone (protocol 1: **Figure 1A**). Medetomidine combined with phenylephrine maintained mean blood pressure (**B**) at the baseline level. Vagotomy partially restored the decrease in heart rate but had no effect on mean blood pressure. **P<0.01; ‡P<0.01 vs. medetomidine alone (protocol 1: **Figure 1A**).

markedly increased dialysate ACh concentration in the medetomidine-treated group (**Figure 5B**). The average slopes of the regression lines between mean BP and log dialysate ACh concentration were 0.0018±0.0004 in the control and 0.0062±0.0006 in the medetomidine-treated group. The slope was significantly steeper in the medetomidine-treated group than that in the control (P<0.01). However, the intercept did not differ significantly between the control (0.59±0.05) and medetomidine-treated (0.68±0.07) groups.

Protocol 4

The 20-Hz electrical stimulation of the right vagal nerve significantly decreased heart rate from 271±11 beats/min at the baseline to 112±6 beats/min and increased dialysate ACh concentration from 7.1±0.9 nmol/L at the baseline to 38.5±7.2 nmol/L (P<0.01). However, both 10 and 100 μg/kg of me-

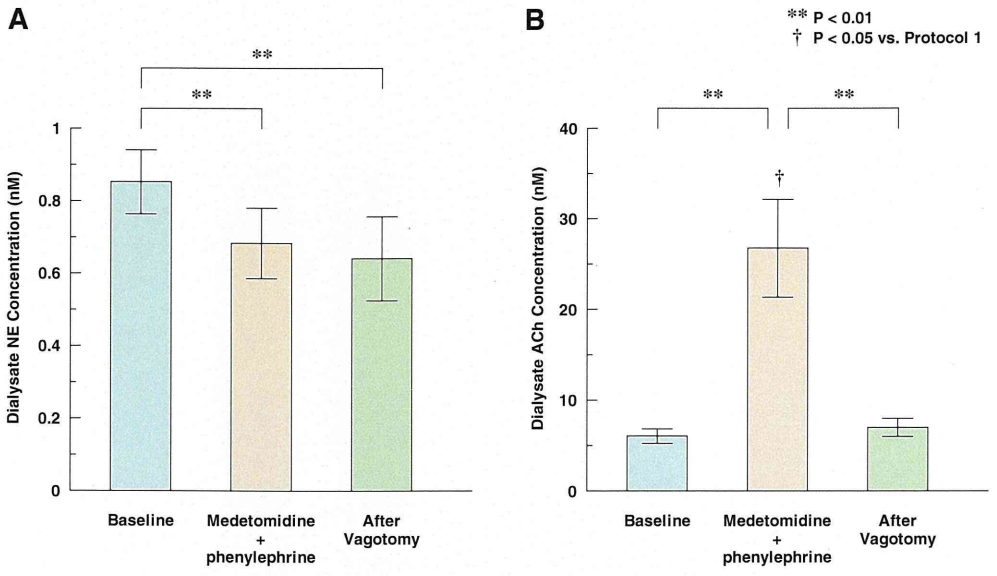

Figure 4. Effects of simultaneous intravenous administration of medetomidine and phenylephrine on dialysate NE (**A**) and ACh concentrations (**B**). Medetomidine combined with phenylephrine decreased dialysate NE concentration (**A**), and the decrease was similar to medetomidine alone (protocol 1: **Figure 2A**). Medetomidine combined with phenylephrine caused a marked increase in dialysate ACh concentration (**B**) and the increase was significantly greater than medetomidine alone (protocol 1: **Figure 2B**). Vagotomy suppressed the increase in dialysate ACh concentration. **P<0.01; †P<0.05 vs. medetomidine alone (protocol 1: **Figure 2B**). ACh, acetylcholine; NE, norepinephrine.

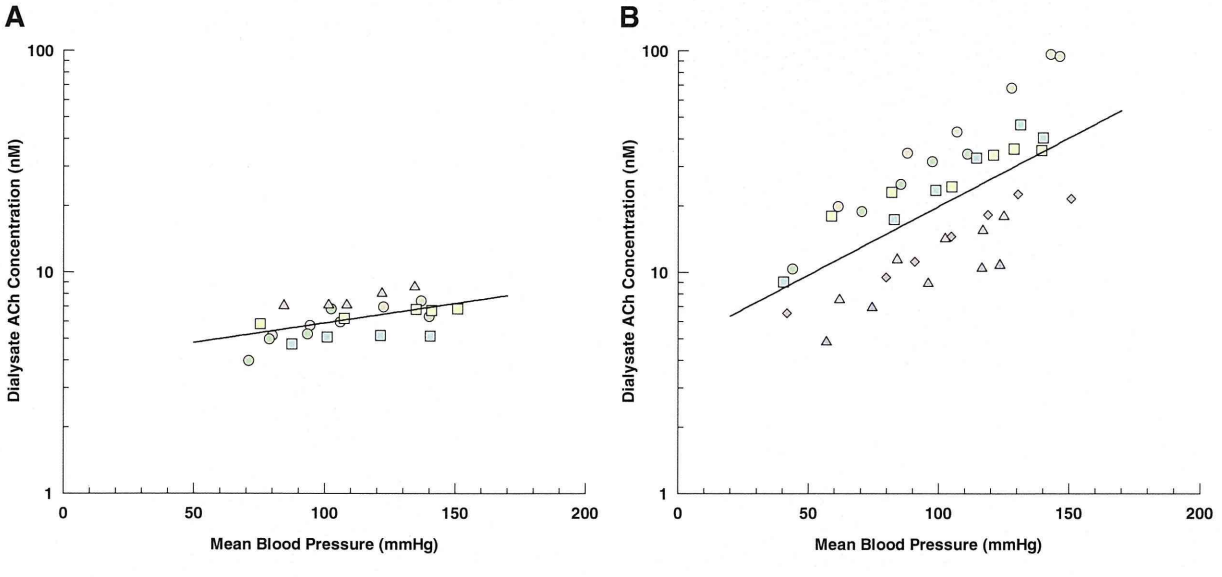

Figure 5. Regression lines of dialysate ACh concentration vs. MBP in control group (**A**) and medetomidine-treated group (**B**). In the control group (n=5), the increase in MBP had little effect on dialysate ACh concentration (**A**). In the medetomidine-treated group (n=7), dialysate ACh concentration was elevated with increase in MBP (**B**). Average regression line for control group: log[ACh]= 0.0018×MBP+0.59. Average regression line for medetomidine-treated group: log[ACh]=0.0062×MBP+0.68. Each symbol represents the data of 1 animal. ACh, acetylcholine; MBP, mean blood pressure.

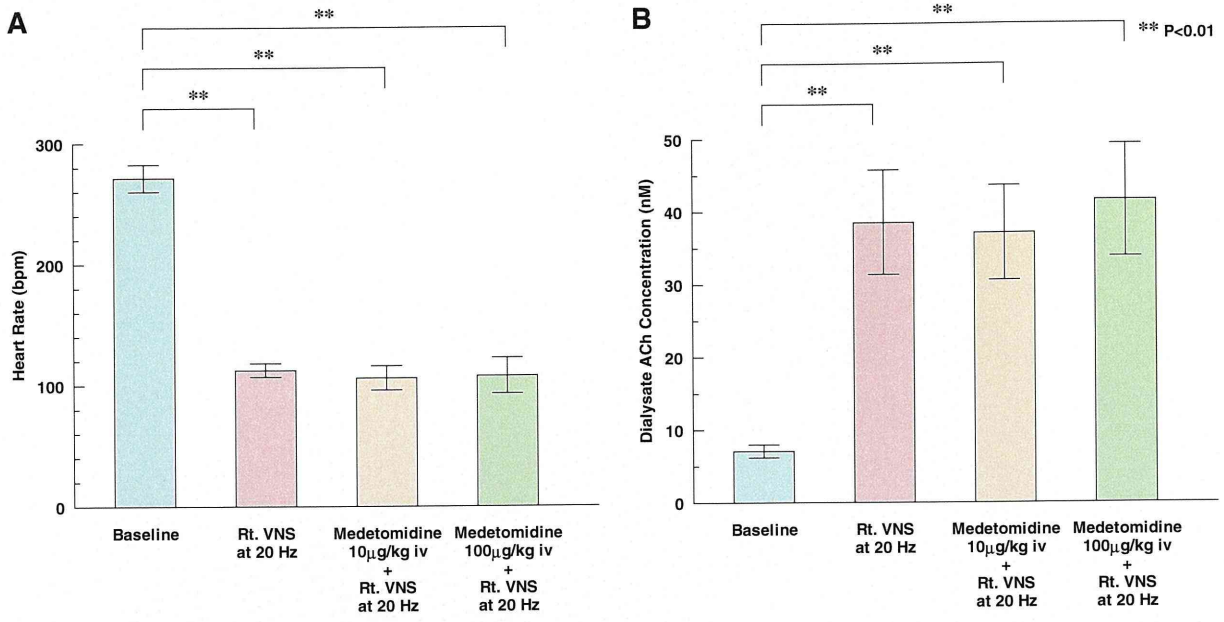

Figure 6. Peripheral effects of medetomidine on heart rate (**A**) and dialysate acetylcholine (ACh) concentration (**B**) under electrical stimulation of the right cervical vagal nerve. The 20-Hz electrical stimulation of the right cervical vagal nerve significantly decreased heart rate and increased dialysate ACh concentration. However, medetomidine did not affect the heart rate and dialysate ACh concentration under electrical vagal nerve stimulation (VNS).

detomidine did not affect heart rate and dialysate ACh concentration under the electrical stimulation (106±9.9 beats/min and 37.1±6.1 nmol/L at 10 μg/kg, 108±15 beats/min and 41.6±7.7 nmol/L at 100 μg/kg).

Discussion

We have elucidated the effects of medetomidine on cardiac sympathetic and vagal nerve activities simultaneously using cardiac microdialysis technique. Intravenous administration of 10 μg/kg of medetomidine significantly decreased sympathetic NE release to the SA node, while intravenous administration of 100 μg/kg of medetomidine significantly increased vagal ACh release to the SA node in addition to sympathetic suppression.

α_2-Adrenergic Agonist and Cardiac Sympathetic Nerve Activity

It is well-documented that α_2-adrenergic agonist suppresses sympathetic nerve activity.[15] Oku et al reported that dexmedetomidine suppressed renal sympathetic nerve discharge in baroreceptor-denervated rabbits.[16] In the present study, low-dose medetomidine decreased heart rate and mean BP through inhibiting sympathetic nerve activity, without affecting cardiac vagal nerve activity. High-dose medetomidine also suppressed NE release to the same level as low-dose medetomidine.

Several mechanisms may be involved in the sympathoinhibitory effect of α_2-adrenergic agonist. The rostral ventrolateral medulla has been reported to serve as an important site in mediating the hypotensive and sedative effects of α_2-adrenergic agonist.[17] McCallum et al reported that the central sympathoinhibitory effects of α_2-adrenoceptor stimulation are augmented by peripheral inhibition of ganglionic transmission.[18] The results obtained from protocol 1 indicate that low-dose medetomidine may induce a vagal-dominant condition through suppression of the cardiac sympathetic nerve without direct activation of the cardiac vagal nerve.

α_2-Adrenergic Agonist and Cardiac Vagal Nerve Activity

Kamibayashi et al reported that the vagus nerve played an important role in the antidysrhythmic effect of dexmedetomidine.[3] However, because it is difficult to selectively monitor cardiac vagal nerve activity, there is little direct evidence that α_2-adrenergic agonists can directly increase cardiac vagal nerve activity. In the present study, high-dose medetomidine significantly decreased heart rate and mean BP compared with low-dose medetomidine in protocol 1, and analyses of NE and ACh release by microdialysis technique proved that these decreases in heart rate and mean BP were associated with an increase in vagal ACh release to the heart. Histocytological studies demonstrated the presence of α_2-adrenergic receptors in the vagal dorsal motor nucleus and nucleus tractus solitarius.[19] Therefore, it is possible that α_2-adrenergic agonists directly activate the cardiac vagal nerve. It is also possible that intravenous medetomidine also modulates vagal ACh release through ganglionic transmission and the direct action to nerve endings. In protocol 4, however, medetomidine did not affect heart rate or the dialysate ACh concentration under electrical stimulation of the right efferent vagal nerve. Thus, in our experimental setting the peripheral effects of medetomidine on cardiac vagal nerve activity may be small compared with its central effects.

To exclude the possibility that medetomidine-induced hypotension affects local ACh concentrations, the mean BP was maintained constant by co-administration of phenylephrine in protocol 2. High-dose medetomidine combined with phenylephrine enhanced the decrease in heart rate and the increase in dialysate ACh concentration without medetomi-

dine-induced hypotension, indicating that hypotension occurring in protocol 1 had actually reduced ACh release in response to high-dose medetomidine. The results also suggest an interaction between baroreflex-induced and medetomidine-induced vagal nerve activation, which was extensively examined in protocol 3. In protocol 3, medetomidine steepened the slope of the regression line between mean BP and log dialysate ACh concentration, without affecting the intercept. In other words, medetomidine enhanced the baroreflex-induced ACh release from cardiac vagal nerve endings. Because the central pathway of baroreflex includes the vagal dorsal motor nucleus and nucleus tractus solitarius, in which α_2-adrenergic receptors have been demonstrated,[19] medetomidine may act on this pathway and modulate baroreflex-induced ACh release.

Clinical Implication

The selective α_2-adrenergic agonist, dexmedetomidine, is widely used for sedation in intensive care units. Bradycardia and hypotension are known to be unfavorable events during dexmedetomidine sedation.[20] Some cases of dexmedetomidine-induced atrioventricular block followed by cardiac arrest have been reported.[21,22] This critical complication may be associated with direct vagal activation by the α_2-adrenergic agonist. Compared with our previous results of electrical cervical vagal nerve stimulation in rabbits,[9] intravenous administration of 100 μg/kg of medetomidine had an effect equivalent to electrical vagal stimulation at 10 Hz. Furthermore, when the mean BP was maintained constant using phenylephrine, medetomidine had a stronger effect on cardiac vagal nerve activity, which is similar to 20-Hz electrical vagal stimulation, and this magnitude may sometimes cause atrioventricular block or sinus arrest.

Notwithstanding these adverse effects, vagal activation has several favorable cardioprotective effects. Our study proved that medetomidine, a selective α_2-adrenergic agonist, is a strong activator of cardiac vagal nerve. Vanoli et al[6] reported that vagal stimulation after acute ischemia can prevent ventricular fibrillation. Ando et al reported that efferent vagal nerve stimulation prevented ischemia-induced arrhythmias by preserving connexin 43 protein.[23] Our results suggest that vagal activation in addition to sympathetic suppression probably contributes to the antiarrhythmic effect of medetomidine.

Because inhibition of the sympathetic nerve system has been the cornerstone of drug therapy for heart failure,[24] a selective α_2-adrenergic agonist may be a potential therapeutic option for heart failure. Recent studies have shown that electrical vagal nerve stimulation also improves the outcomes in patients with heart failure.[25] Electrical stimulation of carotid baroreceptor has recently been reported to be a therapeutic option for heart failure. Sabbah et al reported that chronic electrical stimulation of the carotid sinus baroreflex improved left ventricular function and promoted reversal of ventricular remodeling in dogs with advanced heart failure.[26] Our study demonstrated that medetomidine modulates baroreflex control to enhance vagal nerve activity, which may also induce further cardioprotective effects.

Study Limitations

First, ACh is degraded by ACh esterase immediately after release. Therefore, detection of in vivo ACh release requires the addition of eserine, a specific ACh esterase inhibitor, into the perfusate. The presence of eserine around the semipermeable membrane might have affected ACh release in the vicinity of the semipermeable membrane. Eserine could have activated regulatory pathways such as autoinhibition of ACh release via muscarinic receptors.

Second, medetomidine is a chiral imidazole derivative. Thus, imidazoline receptors may also be involved in the cardiac vagal activation by medetomidine. Further investigation is necessary to clarify the influence of imidazoline receptors on cardiac vagal nerve activity. However, because an α_2-adrenergic antagonist, atipamezole, abolished the hemodynamic responses to medetomidine, we think that the cardiovascular effects of medetomidine are mainly related to the direct action of α_2-adrenergic receptors.

Third, the interactive effects between sympathetic and vagal nerve endings remain uncertain in the present study. Thus, we need further investigations including the open-loop approach where baroreceptor input pressure is strictly controlled.

Conclusion

A selective α_2-adrenergic agonist, medetomidine, directly activates cardiac vagal nerve and enhances the baroreflex control of vagal nerve activity. Medetomidine may be a therapeutic option for life-threatening arrhythmia or heart failure if the adverse effects are properly managed.

Acknowledgments

This study was supported by a research project promoted by the Japanese Ministry of Health, Labour and Welfare (H20-katsudo-Shitei-007 and H21-nano-Ippan-005); Grants-in-Aid for Scientific Research (No. 20390462 and No. 23592319) from the Ministry of Education, Culture, Sports, Science and Technology; the Industrial Technology Research Grant Program from New Energy and Industrial Technology Development Organization (NEDO) of Japan; and Dr Hiroshi Irisawa & Dr Aya Irisawa Memorial Research Grant from the Japan Heart Foundation.

References

1. Hsu YW, Cortinez LI, Robertson KM, Keifer JC, Sum-Ping ST, Moretti EW, et al. Dexmedetomidine pharmacodynamics: Part I: Crossover comparison of the respiratory effects of dexmedetomidine and remifentanil in healthy volunteers. *Anesthesiology* 2004; **101:** 1066–1076.
2. Hayashi Y, Sumikawa K, Maze M, Yamatodani A, Kamibayashi T, Kuro M, et al. Dexmedetomidine prevents epinephrine-induced arrhythmias through stimulation of central alpha 2 adrenoceptors in halothane-anesthetized dogs. *Anesthesiology* 1991; **75:** 113–117.
3. Kamibayashi T, Hayashi Y, Mammoto T, Yamatodani A, Sumikawa K, Yoshiya I. Role of the vagus nerve in the antidysrhythmic effect of dexmedetomidine on halothane/epinephrine dysrhythmias in dogs. *Anesthesiology* 1995; **83:** 992–999.
4. Yamazaki T, Asanoi H, Ueno H, Yamada K, Takagawa J, Kameyama T, et al. Central sympathetic inhibition augments sleep-related ultradian rhythm of parasympathetic tone in patients with chronic heart failure. *Circ J* 2005; **69:** 1052–1056.
5. Lombardi F, Sandrone G, Pernpruner S, Sala R, Garimoldi M, Cerutti S, et al. Heart rate variability as an index of sympathovagal interaction after acute myocardial infarction. *Am J Cardiol* 1987; **60:** 1239–1245.
6. Vanoli E, De Ferrari GM, Stramba-Badiale M, Hull SS Jr, Foreman RD, Schwartz PJ. Vagal stimulation and prevention of sudden death in conscious dogs with a healed myocardial infarction. *Circ Res* 1991; **68:** 1471–1481.
7. Schwartz PJ, La Rovere MT, Vanoli E. Autonomic nervous system and sudden cardiac death: Experimental basis and clinical observations for post-myocardial infarction risk stratification. *Circulation* 1992; **85:** I77–I91.
8. Kuusela E, Raekallio M, Anttila M, Falck I, Mölsä S, Vainio O. Clinical effects and pharmacokinetics of medetomidine and its enantiomers in dogs. *J Vet Pharmacol Ther* 2000; **23:** 15–20.
9. Shimizu S, Akiyama T, Kawada T, Shishido T, Yamazaki T, Kamiya A, et al. In vivo direct monitoring of vagal acetylcholine release to the sinoatrial node. *Auton Neurosci* 2009; **148:** 44–49.
10. Shimizu S, Akiyama T, Kawada T, Shishido T, Mizuno M, Kamiya A, et al. In vivo direct monitoring of interstitial norepinephrine levels at the sinoatrial node. *Auton Neurosci* 2010; **152:** 115–118.
11. Shimizu S, Akiyama T, Kawada T, Sonobe T, Kamiya A, Shishido T, et al. Centrally administered ghrelin activates cardiac vagal nerve

in anesthetized rabbits. *Auton Neurosci* 2011; **162:** 60–65.
12. Akiyama T, Yamazaki T, Ninomiya I. In vivo monitoring of myocardial interstitial norepinephrine by dialysis technique. *Am J Physiol* 1991; **261:** H1643–H1647.
13. Akiyama T, Yamazaki T, Ninomiya I. In vivo detection of endogenous acetylcholine release in cat ventricles. *Am J Physiol* 1994; **266:** H854–H860.
14. Glantz SA. Primer of biostatistics, 6th edn. New York: McGraw-Hill, 2005.
15. Heusch G, Schipke J, Thämer V. Clonidine prevents the sympathetic initiation and aggravation of poststenotic myocardial ischemia. *J Cardiovasc Pharmacol* 1985; **7:** 1176–1182.
16. Oku S, Benson KT, Hirakawa M, Goto H. Renal sympathetic nerve activity after dexmedetomidine in nerve-intact and baroreceptor-denervated rabbits. *Anesth Analg* 1996; **83:** 477–481.
17. Yamazato M, Sakima A, Nakazato J, Sesoko S, Muratani H, Fukiyama K. Hypotensive and sedative effects of clonidine injected into the rostral ventrolateral medulla of conscious rats. *Am J Physiol Regul Integr Comp Physiol* 2001; **281:** R1868–R1876.
18. McCallum JB, Boban N, Hogan Q, Schmeling WT, Kampine JP, Bosnjak ZJ. The mechanism of alpha2-adrenergic inhibition of sympathetic ganglionic transmission. *Anesth Analg* 1998; **87:** 503–510.
19. Robertson HA, Leslie RA. Noradrenergic alpha 2 binding sites in vagal dorsal motor nucleus and nucleus tractus solitarius: Autoradiographic localization. *Can J Physiol Pharmacol* 1985; **63:** 1190–1194.
20. Candiotti KA, Bergese SD, Bokesch PM, Feldman MA, Wisemandle W, Bekker AY; MAC Study Group. Monitored anesthesia care with dexmedetomidine: A prospective, randomized, double-blind, multicenter trial. *Anesth Analg* 2010; **110:** 47–56.
21. Nagasaka Y, Machino A, Fujikake K, Kawamoto E, Wakamatsu M. Cardiac arrest induced by dexmedetomidine. *Masui* 2009; **58:** 987–989.
22. Ingersoll-Weng E, Manecke GR Jr, Thistlethwaite PA. Dexmedetomidine and cardiac arrest. *Anesthesiology* 2004; **100:** 738–739.
23. Ando M, Katare RG, Kakinuma Y, Zhang D, Yamasaki F, Muramoto K, et al. Efferent vagal nerve stimulation protects heart against ischemia-induced arrhythmias by preserving connexin43 protein. *Circulation* 2005; **112:** 164–170.
24. Sata Y, Krum H. The future of pharmacological therapy for heart failure. *Circ J* 2010; **74:** 809–817.
25. Schwartz PJ. Vagal stimulation for heart diseases: From animals to men: An example of translational cardiology. *Circ J* 2010; **75:** 20–27.
26. Sabbah HN, Gupta RC, Imai M, Irwin ED, Rastogi S, Rossing MA, et al. Chronic electrical stimulation of the carotid sinus baroreflex improves left ventricular function and promotes reversal of ventricular remodeling in dogs with advanced heart failure. *Circ Heart Fail* 2011; **4:** 65–70.

J Appl Physiol 111: 1614–1621, 2011.
First published September 15, 2011; doi:10.1152/japplphysiol.00501.2011.

Interaction between vestibulo-cardiovascular reflex and arterial baroreflex during postural change in rats

Chikara Abe,[1] Toru Kawada,[2] Masaru Sugimachi,[2] and Hironobu Morita[1]

[1]*Department of Physiology, Gifu University Graduate School of Medicine, Gifu; and* [2]*Department of Cardiovascular Dynamics, National Cerebral and Cardiovascular Center Research Institute, Suita, Japan*

Submitted 25 April 2011; accepted in final form 8 September 2011

Abe C, Kawada T, Sugimachi M, Morita H. Interaction between vestibulo-cardiovascular reflex and arterial baroreflex during postural change in rats. *J Appl Physiol* 111: 1614–1621, 2011. First published September 15, 2011; doi:10.1152/japplphysiol.00501.2011.—To examine a cooperative role for the baroreflex and the vestibular system in controlling arterial pressure (AP) during voluntary postural change, AP was measured in freely moving conscious rats, with or without sinoaortic baroreceptor denervation (SAD) and/or peripheral vestibular lesion (VL). Voluntary rear-up induced a slight decrease in AP (−5.6 ± 0.8 mmHg), which was significantly augmented by SAD (−14.7 ± 1.0 mmHg) and further augmented by a combination of VL and SAD (−21 ± 1.0 mmHg). Thus we hypothesized that the vestibular system sensitizes the baroreflex during postural change. To test this hypothesis, open-loop baroreflex analysis was conducted on anesthetized sham-treated and VL rats. The isolated carotid sinus pressure was increased stepwise from 60 to 180 mmHg while rats were placed horizontal prone or in a 60° head-up tilt (HUT) position. HUT shifted the carotid sinus pressure-sympathetic nerve activity (SNA) relationship (neural arc) to a higher SNA, shifted the SNA-AP relationship (peripheral arc) to a lower AP, and, consequently, moved the operating point to a higher SNA while maintaining AP (from 113 ± 5 to 114 ± 5 mmHg). The HUT-induced neural arc shift was completely abolished in VL rats, whereas the peripheral arc shifted to a lower AP and the operating point moved to a lower AP (from 116 ± 3 to 84 ± 5 mmHg). These results indicate that the vestibular system elicits sympathoexcitation, shifting the baroreflex neural arc to a higher SNA and maintaining AP during HUT.

arterial baroreflex; arterial pressure; sympathetic nerve activity; head-up tilt; rear-up; neural arc; peripheral arc

DAILY ACTIVITY-INDUCED CHANGES in the gravitational vector are one of the major disturbances that affect the cardiovascular system (43). For example, a postural change from a recumbent to an upright position induces an increase in the hydrostatic pressure gradient, a footward fluid shift, reduced venous return and cardiac output, and reduced arterial pressure (AP). This reduction in AP is sensed by baroreceptors in the blood vessels, and AP is thought to be stabilized by the arterial baroreflex, an important negative feedback process (6, 37). Alternatively, postural changes might stimulate the vestibular organ, which is also thought to be involved in AP regulation with postural change (8, 17, 30, 39). AP maintenance during passive postural change was found to be dependent on the vestibular system: if the vestibular system was not functioning properly, AP decreased or fluctuated. However, the role of the vestibular system in maintaining AP during a voluntary postural change remains unclear, since most previous experiments studied passive postural change using a tilt table. Therefore, one of the aims of this study was to examine the role of the vestibular system in maintaining AP during a voluntary postural change in conscious rats. This is important for considering the role of the vestibular system in maintaining AP during daily activity. We tested the hypothesis that the vestibular system plays a significant role in AP maintenance during voluntary rear-up behavior in rats.

Stimulation of the vestibular system by head movement or changes in gravitational forces is known to induce sympathoexcitation (2, 11, 23, 33). Although sympathoexcitation was observed during postural change (10, 18, 31), it is not clear whether it is mediated through the vestibular system. Postural change-induced AP decrease might also induce sympathoexcitation through the arterial baroreflex. In this regard, Ray (33) performed an elegant experiment demonstrating that lower body negative pressure, which is a result of postural change-induced footward fluid shift, induces an increase in sympathetic nerve activity (SNA); a further increase in SNA was observed by head-down rotation. This result strongly suggests that the observed sympathoexcitation upon postural change might be a sum of the baroreflex-mediated and the vestibular-mediated sympathoexcitation. Thus it is possible that vestibular-mediated sympathoexcitation modulates arterial baroreflex function during postural change. Anatomic and functional convergence of vestibular and baroreceptor signaling to the nucleus tractus solitarius further supports the idea of interaction between the vestibular system and arterial baroreflex (4, 28, 45). However, functional interaction between the baroreflex and the vestibular system during postural change has not been quantitatively analyzed. Therefore, the second aim of the present study was to quantitatively analyze the functional interaction between the baroreflex and the vestibular system during postural change. We tested the hypothesis that the vestibulo-sympathetic reflex sensitizes the arterial baroreflex during postural change.

To address the first aim, the AP response during voluntary rear-up behavior was measured in rats with or without a peripheral vestibular organ and/or arterial baroreceptors. To address the second aim, we evaluated the arterial baroreflex functional curve in an open-loop experiment with isolated carotid sinus baroreceptor regions during prone and 60° head-up tilt (HUT) positions in sham-treated vestibular-intact (sham) and vestibular-lesioned (VL) rats.

METHODS

Animals. The animals used in the study were maintained in accordance with the "Guiding Principles for the Care and Use of Animals in the Field of Physiological Science" set by the Physiological Society of Japan. The experiments were approved by the Animal Research

Address for reprint requests and other correspondence: H. Morita, Dept. of Physiology, Gifu Univ. Graduate School of Medicine, 1-1 Yanagido, Gifu 501-1194, Japan (e-mail: zunzunmorita@gmail.com).

Committee of Gifu University and by the Animal Subjects Committee of the National Cerebral and Cardiovascular Center, Japan. Male Sprague-Dawley rats ($n = 42$), weighing 230–250 g (8 wk old), were used for the experiments.

AP measurement in conscious rats. To examine the role of the vestibular system and/or sinoaortic baroreflex in AP regulation during voluntary rear-up behavior, AP was continuously measured for 48 h in chronically implanted conscious rats. Four groups of rats were examined: sham group ($n = 7$), in which both the sinoaortic baroreceptors and vestibular organs were intact; VL group ($n = 7$), in which the sinoaortic baroreceptors were intact, but the vestibular organs were lesioned; sinoaortic baroreceptor denervation (SAD) group ($n = 7$), in which the sinoaortic baroreceptors were denervated, but the vestibular organs were intact; and SAD+VL group ($n = 7$), in which both the sinoaortic baroreceptors and vestibular organs were lesioned. The following operations were performed to prepare these groups of rats.

Ten days before the experiment, all rats were anesthetized with pentobarbital sodium (50 mg/kg), and the following operations were performed. *1*) The abdominal aorta was exposed via a midline laparotomy for rats in all groups. The catheter portion of the telemetry transmitter probe for AP measurements (PA-C40; Data Science International, St Paul, MN) was inserted into the abdominal aorta. The tip of the catheter was set distal to the renal artery bifurcation. The probe was then sutured to the abdominal wall, and the incision was closed. *2*) In the VL and SAD+VL rats, sodium arsanilate solution (100 mg/ml) was injected into the bilateral middle ear cavities (50 μl/ear). Although the histological verification was not performed in the present study, previous study from our laboratory has proved that this VL method could completely destroy the epithelial cells (1). As a control, saline, instead of sodium arsanilate solution, was injected into the sham and SAD rats. *3*) In the SAD and SAD+VL rats, the aortic depressor nerve was isolated and dissected with a midcervical incision, the carotid sinus was isolated from the surrounding connective tissues, and 10% phenol in ethanol was applied. In the sham and VL rats, a midcervical incision was made, but the aortic depressor nerves and carotid sinus were left intact as a control. *4*) A polyethylene catheter (PE-50; Becton Dickinson, Sparks, MD) was inserted into the inferior vena cava via the left femoral vein to confirm the completeness of SAD using a phenylephrine injection 2 days after surgery. In rats with SAD, phenylephrine-induced bradycardia was completely abolished. This polyethylene catheter was removed after the confirmation of SAD under gas anesthesia with enflurane (Abbott Japan, Osaka, Japan).

All of the rats were maintained in their individual cages to recover from surgery until the day of the experiment. Penicillin G potassium (6,000 U/day) and buprenorphine (3 μg/kg) were injected intramuscularly for 3 days after surgery. At 5 days postsurgery, the swimming test was performed to confirm the completion of VL. Rats were gently put on the surface of tepid water, and swimming behavior was observed. Sham rats could swim and reached the edge of water bath (27 cm width × 40 cm length × 20 cm depth); however, VL rats were unable to determine the direction in which they had to swim to reach the water surface and continued to turn around under the water (14).

On the day of the experiment, each rat was placed in an individual cage (20 cm width × 36 cm length × 22 cm height). Infrared sensors (NA2-N16D; SUNX, Aichi, Japan) were aligned horizontally at a height of 15 cm from the floor of the cage. The AP signal was received by a PhysioTel Receiver (RLA 1020; Data Science International), and the output was relayed through a calibrated pressure output adapter (R11CPA; Data Science International) and a dual ambient pressure monitor (C11PR; Data Science International). The AP and the signal from the infrared sensor were recorded using an analog-to-digital converter (PowerLab; AD instruments, Bella Vista, NSW, Australia) at a rate of 100 Hz. Video pictures from a video camera (DCR-TRV70; Sony, Tokyo, Japan) were also synchronized with the digital data. All of the rats were fed ad libitum, the cages were maintained on a 12:12-h light-dark cycle, and the room temperature was maintained at 24 ± 1°C. If the infrared signal was on for more than 15 s, the video picture was checked to see whether that behavior was related to drinking, because drinking behavior itself affects AP (13, 41). We defined rear-up behavior as rear-up (>15 s) without drinking. The minimum number of rear-ups lasting for more than 15 s was 30 for two SAD+VL rats; therefore, we randomly selected 30 rear-up events (Rnd function of Excel VBA) for each rat in all groups, and these data were averaged.

Measurement of baroreflex gain under open-loop conditions. Operations to generate the sham ($n = 7$) and VL ($n = 7$) rats were performed 5 days before the experiment. Anesthesia was induced using enflurane (Abbott Japan, Osaka, Japan) inhalation via a face mask. Sodium arsanilate solution (100 mg/ml) or saline was injected into the bilateral middle ear cavities (50 μl/ear) of VL and sham rats, respectively. Penicillin G potassium (6,000 U/day) was injected intramuscularly for 3 days after surgery.

On the day of the experiment, each rat was anesthetized with an intraperitoneal injection (2 ml/kg) of a mixture of urethane (500 mg/ml) and α-chloralose (50 mg/ml) and mechanically ventilated (SAR830/P; CWE, Ardmore, PA) through a tracheal tube with oxygen-enriched room air. A venous catheter was inserted into the left femoral vein, and a mixed solution [1 ml of the mixed urethane and α-chloralose solution, 2 ml of pancuronium bromide (Myoblock, Sankyo, Tokyo, Japan), and 47 ml of Ringer solution] was administered continuously (5 $ml \cdot kg^{-1} \cdot h^{-1}$). An arterial catheter was inserted into the left femoral artery to measure AP. Heart rate (HR) was calculated from the AP waveform. To record SNA, the postganglionic renal sympathetic nerve was isolated through a right or left flank incision, and two stainless-steel electrodes (AS633; Cooner Wire, Chatsworth, CA) were placed around it. The nerve and electrodes were covered and fixed with silicone gel (Kwik-Sil; World Precision Instruments).

The vagal and aortic nerves were sectioned bilaterally at the neck, avoiding the reflexes from the cardiopulmonary region and the aortic arch. The carotid sinus regions were isolated bilaterally from the systemic circulation, according to previously reported procedures (36, 38). Briefly, a 7–0 polypropylene suture with a fine needle (Prolene, Ethicon) was passed through the tissue between the external and internal carotid arteries, and the external carotid artery was ligated close to the carotid bifurcation. The internal carotid artery was embolized with two to three steel balls (0.8 mm diameter; Tsubaki Nakashima, Nara, Japan) injected into the common carotid artery. Under these conditions, the brain stem area was perfused using the bilateral vertebral arteries. The isolated carotid sinuses were filled with warmed Ringer solution through catheters inserted into the common carotid arteries. Carotid sinus pressure (CSP) was regulated with a servo-controlled piston pump. Heparin sodium (100 U/kg) was given intravenously to prevent blood coagulation. Body temperature was maintained at ~37°C with a heating pad.

After the surgical procedures were completed, the rat was fixed on a tilt table with the maxillary incisal teeth anchor. All signals were recorded using an analog-to-digital converter (PowerLab; AD instruments) at a rate of 1,000 Hz. To estimate the static input-output relationship of the carotid sinus baroreflex, the CSP was set to 60 mmHg for 4–6 min and then increased stepwise from 60 to 180 mmHg in increments of 20 mmHg per 30 s. This procedure was repeated three times in the prone horizontal position and three times in the HUT position. At the end of the experiment, we confirmed the disappearance of SNA in response to an intravenous bolus injection of a ganglionic blocker, hexamethonium bromide (60 mg/kg), and recorded the noise level, which was treated as the zero level of SNA. Because the absolute voltage of SNA varied among the animals, depending on the recording conditions, the average SNA during the last 10 s at a CSP level of 60 mmHg in the prone horizontal position was defined as 100%. To quantify the open-loop static characteristics of the carotid sinus baroreflex, the mean SNA and AP were obtained during the last 10 s at each CSP level of the stepwise input protocol.

Table 1. *Means ± SE for AP, HR, and AP variability for each group*

Group	*n*	AP, mmHg	HR, beats/min	Variability, mmHg
Sham	7	96 ± 2	412 ± 4	7.1 ± 0.4
VL	7	97 ± 2	409 ± 3	7.4 ± 0.2
SAD	7	96 ± 3	403 ± 2	18.5 ± 1.2*
SAD+VL	7	97 ± 1	408 ± 4	17.8 ± 0.7*

Values are means ± SE; *n*, no. of rats. Arterial pressure (AP) and heart rate (HR) were measured for 12 h and averaged every 5 s to obtain individual baseline values and then averaged to obtain the group mean ± SE. Variability is the standard deviation of AP. Sham, vestibular intact; VL, vestibular lesioned; SAD, sinoaortic baroreceptor denervated. *$P < 0.05$ vs. sham or VL.

The static characteristics of the baroreflex neural arc (relationship between CSP and SNA) and the total baroreflex (relationship between CSP and AP) were described by fitting four-parameter logistic functions to the input-output data as follows (20, 22):

$$y = P_1/\{1 + \exp[P_2 \times (x - P_3)]\} + P_4$$

where x and y denote the input (CSP) and output (SNA or AP), respectively; P_1 is the response range of the output; P_2 is the slope coefficient; P_3 is the midpoint pressure of the input; and P_4 is the minimum value for the output. For convenience, the maximum gain of the logistic function is reported by a positive value as $P_1 \times P_2/4$.

The static characteristics of the baroreflex peripheral arc (relationship between SNA and AP) were quantified from a scatter plot. A linear regulation line is represented as follows:

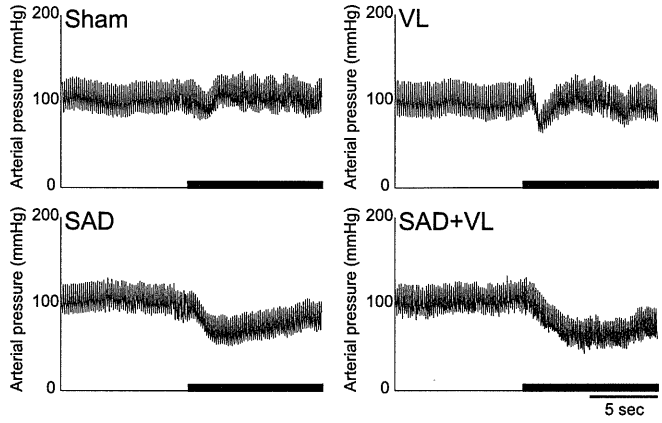

Fig. 2. Typical recordings of arterial pressure (AP) in response to rear-up in vestibular-intact (sham), VL, SAD, and SAD+VL rats. The thick horizontal bar indicates the rear-up period.

$$AP = a \times SNA + b$$

where a and b represent the slope and intercept, respectively.

Statistical analysis. All data are presented as means ± SE. For the data presented in Table 1 and Fig. 3*B*, one-way ANOVA was applied. Repeated-measures two-way ANOVA was used for the data presented in Table 2. If the *F*-ratio indicated statistical significance, the Tukey-Kramer post hoc test was applied for between-group comparisons. A simple linear regression line was calculated using the least squares method for the peripheral arc of Fig. 5*B*, and the analysis of covari-

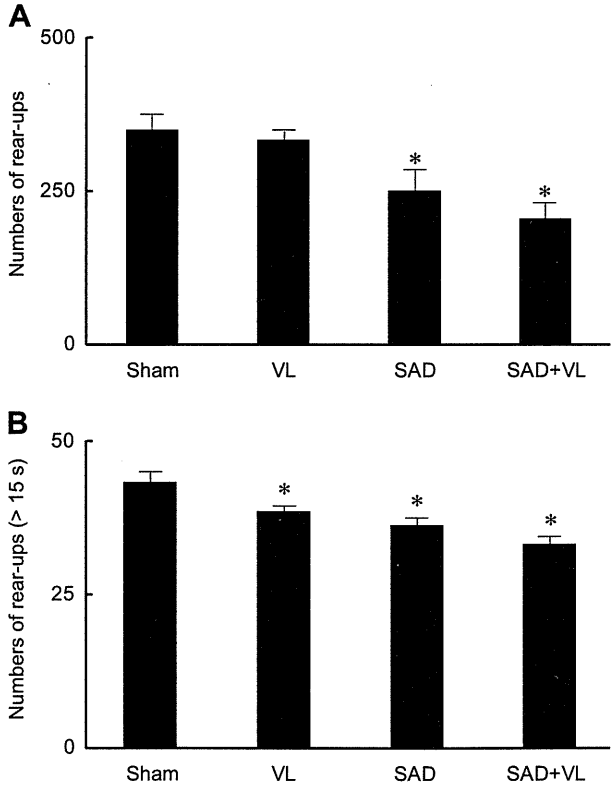

Fig. 1. Summarized data for the total number of rear-ups without drinking during the 12-h dark period (*A*), and rear-ups lasting for more than 15 s (*B*) in the sham-treated (sham), vestibular-lesioned (VL), sinoaortic baroreceptor-denervated (SAD), and SAD+VL rats. Values are means ± SE. *$P < 0.05$ vs. sham.

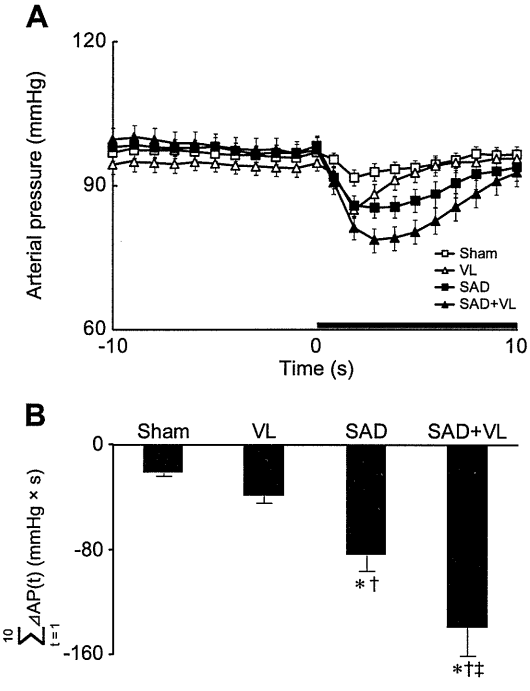

Fig. 3. *A*: average AP response to rear-up behavior in vestibular-intact (sham), VL, SAD, and SAD+VL rats. Thirty data points measuring AP induced by rear-up exceeding 15 s were randomly selected from the individual rats and then averaged for each group. The thick horizontal bar indicates the rear-up period. *B*: summarized data for the sum of the differences in AP ($\sum\Delta AP$) between each time point (t; 1–10 s) during rear-up and the mean value for the 10 s before rear-up. If the difference was positive, the value was considered to be zero. Values are means ± SE. *$P < 0.05$ vs. sham rats. †$P < 0.05$ vs. VL rats. ‡$P < 0.05$ vs. SAD rats.

ance method was applied. In all tests, $P < 0.05$ was considered statistically significant.

RESULTS

To determine whether the vestibular system and/or sinoaortic baroreflex is required for AP regulation during voluntary rear-up behavior, the AP of sham, SAD, VL, and SAD+VL rats was measured. Table 1 shows the mean baseline AP, HR, and AP variability of all of the groups in the experiment. Baseline AP and HR were measured for the 12-h dark period and averaged every 5 s. AP variability is the standard deviation of AP for the 12 h of the dark period. There were no differences in baseline AP or HR among the groups, but a significant increase in AP variability was observed in the SAD and SAD+VL rats compared with both sham and VL rats.

Although there was no obvious difference in the rear-up behavior among groups (supplemental video file; the online version of this article contains supplemental data), the number of rear-ups was affected in the VL and SAD+VL rats compared with sham (Fig. 1*A*). The sham and VL rats reared up ~350 times during the 12-h dark period, which was significantly reduced in the SAD and SAD+VL rats. Furthermore, the number of rear-ups lasting more than 15 s was significantly reduced in the VL, SAD, and SAD+VL rats compared with sham rats (Fig. 1*B*).

Figure 2 shows typical recordings of AP during rear-up behavior in sham, VL, SAD, and SAD+VL rats. AP response during rear-up behavior is summarized in Fig. 3 for all groups. In the sham rats, AP levels changed very little during rear-up (−5.6 ± 0.8 mmHg; Fig. 3*A*). A transient drop in AP (−9.4 ± 0.6 mmHg) was observed at the onset of rear-up in VL rats, but values quickly recovered to the baseline level. In the SAD rats, the reduction in AP was large (−14.7 ± 1.0 mmHg), and recovery was delayed. This tendency was clearly seen in the SAD+VL rats, in which AP decreased by 21 ± 1.0 mmHg, and its recovery was delayed. For statistical analysis, the sum of the differences ($\sum\Delta$) between the 10-s averaged data before rear-up and at each time point during rear-up (from 1 to 10 s) was calculated (Fig. 3*B*). SAD significantly increased $\sum\Delta$AP compared with the sham rats. VL alone had no significant effect on $\sum\Delta$AP, whereas additional VL to SAD significantly increased $\sum\Delta$AP compared with the SAD rats. $\sum\Delta$AP in the SAD+VL rats (131 mmHg × s) was greater than the simple sum of $\sum\Delta$AP in VL and SAD (111 mmHg × s).

Typical recordings of the measurement of baroreflex gain under open-loop conditions are shown in Fig. 4. A stepwise increase in CSP reduced AP, HR, and SNA in both the prone and HUT positions in sham rats. When CSP was 60 mmHg, an increase in SNA was observed in a sham rat, but not in a VL rat.

Figure 5 summarizes the open-loop static characteristics of the carotid sinus baroreflex in the sham and VL rats in the prone and HUT positions. Each parameter is summarized in Table 2. Figure 5*A* shows the baroreflex neural arc of the sham and VL rats in the prone and HUT positions. In the sham rats, the response range of SNA (P_1) was significantly increased by HUT, but the minimum SNA (P_4) did not change, so the increase in the response range was mainly directed to a higher SNA level. SNA levels were similar in VL rats in the prone and HUT positions. Therefore, the response range in the sham HUT

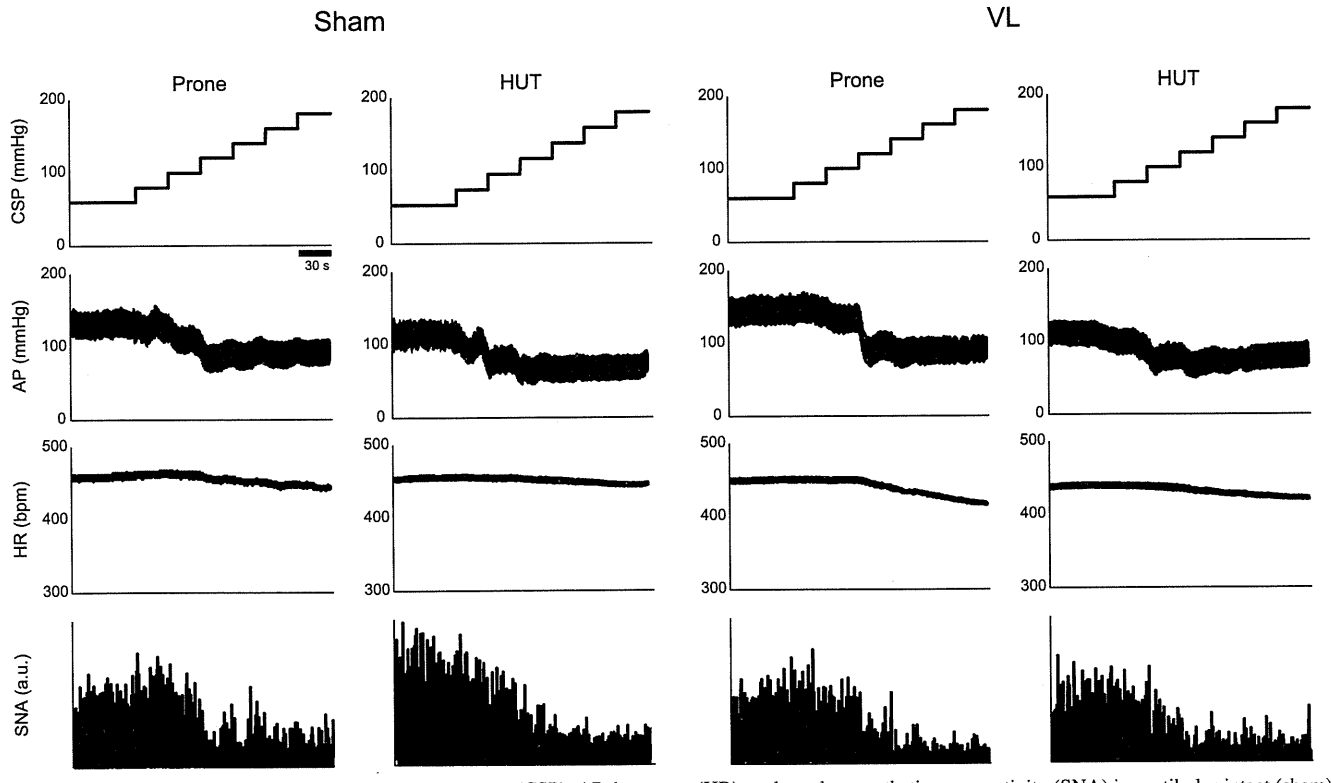

Fig. 4. Representative recordings of the carotid sinus pressure (CSP), AP, heart rate (HR), and renal sympathetic nerve activity (SNA) in vestibular-intact (sham) and VL rats in prone and head-up tilt (HUT) positions. bpm. Beats/min; a.u., arbitrary units.

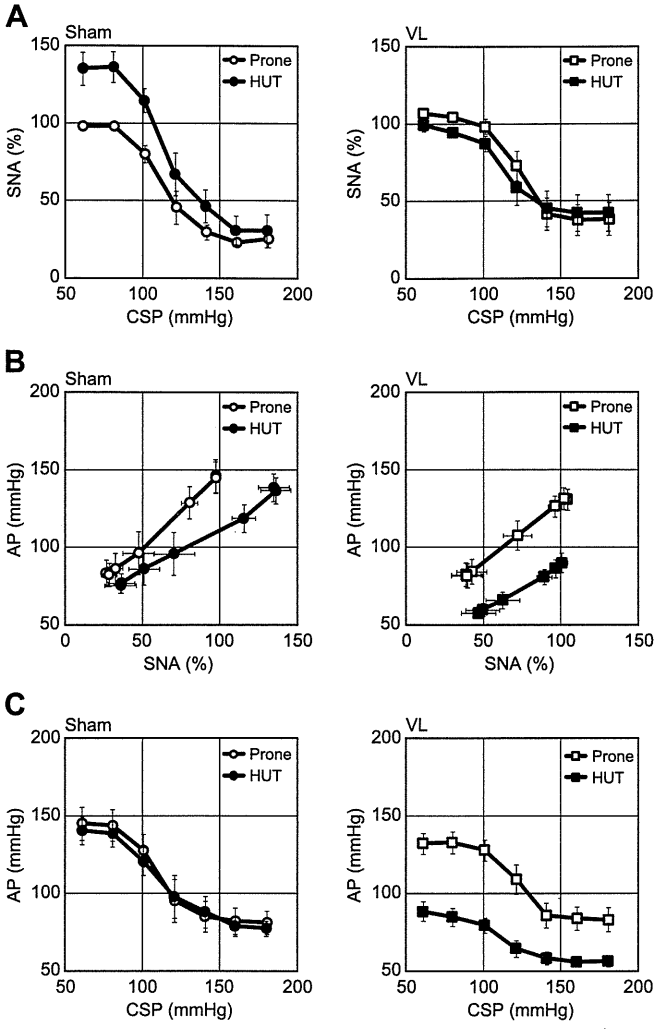

Fig. 5. Static characteristics of the average carotid sinus baroreflex for vestibular-intact (sham) and VL rats in the prone and HUT positions. Static characteristics of the baroreflex neural arc (*A*), baroreflex peripheral arc (*B*), and total baroreflex (*C*) are shown for sham (*left*) and VL (*right*) rats. Values are means ± SE.

rats was significantly larger than that in the VL HUT rats. Neither the maximum gain nor midpoint pressure was affected by VL or HUT (Table 2).

Analysis of covariance in the peripheral arc showed that there was no difference between the sham and VL rats in the prone position, whereas the line was shifted to a lower AP level during HUT in both the sham and VL rats (Fig. 5*B* and Table 2). The degree of shift was significantly larger in the VL rats than in the sham rats.

In the sham rats, the total baroreflex functional curve was not affected by HUT, nor was it affected by VL in the prone position (Fig. 5*C* and Table 2). However, HUT shifted the total functional curve to a lower AP level in the VL rats, with a significant reduction in the response range (P_1), minimum AP (P_4), and maximum gain.

The baroreflex equilibrium diagram was generated by plotting the neural and peripheral arcs on the pressure-SNA plane (Fig. 6). The ordinate is either CSP (the neural arc) or AP (the peripheral arc). The intersection between the neural and peripheral arcs gives the closed-loop operating points. The AP of the operating point was maintained in the sham rats during HUT, with an increase in SNA. In other words, the operating point shifted toward higher SNA levels, with maintenance of AP. However, in the VL rats, the operating point shifted to lower AP levels during HUT.

DISCUSSION

The major findings of the present study are as follows. *1*) The rear-up-induced reduction in AP was increased by SAD alone, but not VL alone; however, VL and SAD together significantly increased the rear-up-induced reduction in AP. *2*) The neural arc was shifted to a higher SNA level by HUT in the sham rats; this shift was not observed in the VL rats. *3*) A downward shift of the peripheral arc was observed in the sham and VL rats during HUT; the magnitude of this shift was greater in the VL rats than in the sham rats. *4*) The operating point of AP was maintained in the sham rats during HUT, but it was significantly reduced in the VL rats.

It is well accepted that the baroreflex plays a significant role in AP regulation during postural changes in humans and animals (9, 25, 37). However, the postural change-induced AP response in SAD animals is still controversial. In anesthetized SAD cats, a large and sustained reduction in AP was observed during HUT (6). In contrast, no difference in the AP response to rear-up behavior was observed between sham and SAD conscious rats (42). The difference in these two studies might be attributable to the use of anesthesia, passive or voluntary postural changes, and/or species differences. In the present study, a significantly larger reduction in AP was observed in conscious SAD rats than in sham rats. Two possibilities can be considered to explain this discrepancy. First, the AP response to rear-up with drinking was omitted from our data because drinking behavior increases AP (13, 41). Alternatively, the pressor response to drinking behavior may have obscured the depressor response to rear-up behavior in the SAD rats, as the drinking-behavior-induced pressor response was larger in the SAD rats than in the sham rats, because there was no buffering system (our unpublished data). Second, the AP variability in the SAD rats was 18.5 ± 1.2 mmHg in the present study, and this value is larger than that reported in the previous rat study (11.7 ± 1.5 mmHg) (42). It is possible that the quality of SAD was different between the two studies.

Passive HUT has been used to examine the role of the vestibular system in AP maintenance during postural changes (8, 17, 30, 39). The present study is the first to examine the role of the vestibular system in AP regulation during voluntary rear-up behavior, under which conditions the lower limb muscle is contracted. This muscle contraction might induce an increase in the venous return and then counteract rear-up-induced AP reduction (26). Furthermore, the muscle-contraction-induced proprioceptive reflex, the somatosensory reflex, and the behavior-linked central command might also counteract reduction in AP (5, 24, 27, 44). Under these conditions, VL alone had no significant effect on rear-up-induced AP reduction; however, in conjunction with an inoperable baroreflex, VL induced a larger reduction in AP compared with SAD alone. The reduction in AP seen in rats with VL or SAD alone was increased by additional denervation. Therefore, the vestibulo-cardiovascular reflex and the baroreflex might operate

Table 2. *Parameters representing the static characteristics of the carotid sinus baroreflex*

	Sham (n = 7)		VL (n = 7)	
	Prone	HUT	Prone	HUT
		Neural arc		
P_1, response range, %	70 ± 6	104 ± 15*	63 ± 8	53 ± 10†
P_2, slope coefficient, mmHg^{-1}	0.32 ± 0.15	0.14 ± 0.03	0.16 ± 0.02	0.14 ± 0.01
P_3, midpoint pressure, mmHg	113 ± 5	117 ± 5	123 ± 3	117 ± 4
P_4				
Minimum SNA, %	28 ± 3	36 ± 9	41 ± 9	46 ± 11
Maximum gain, %/mmHg	5.0 ± 1.9	3.7 ± 0.7	2.5 ± 0.4	1.8 ± 0.4
		Peripheral arc		
R^2	0.67	0.68	0.48	0.43
Regression line	$y = 0.88x + 59.6$	$y = 0.54x + 61.7$*	$y = 0.57x + 66.7$†	$y = 0.35x + 46.3$*†
		Total baroreflex		
P_1, response range, mmHg	60 ± 8	61 ± 10	47 ± 5	30 ± 5†
P_2, slope coefficient, mmHg^{-1}	0.16 ± 0.02	0.18 ± 0.06	0.18 ± 0.02	0.14 ± 0.02
P_3, midpoint pressure, mmHg	112 ± 4	116 ± 7	122 ± 3	113 ± 4
P_4				
Minimum AP, mmHg	86 ± 7	80 ± 5	85 ± 7	58 ± 3*†
Maximum gain	2.3 ± 0.4	2.3 ± 0.4	2.0 ± 0.2	0.9 ± 0.1*†
		Equilibrium diagram		
Operating point AP, mmHg	113 ± 5	114 ± 5	116 ± 3	84 ± 5*†
Operating point SNA, %	60 ± 5	97 ± 7*	82 ± 8†	95 ± 4

Values are means ± SE; n, no. of rats. HUT, head-up tilt; SNA, sympathetic nerve activity. *$P < 0.05$, comparing HUT to prone in the same group. †$P < 0.05$, comparing VL to sham in the same position.

separately, and these two systems might be involved in a functional interaction. This putative interaction was quantitatively analyzed in the anesthetized sham and VL rats using an open-loop baroreflex analysis.

HUT shifted the neural arc to a higher SNA level and shifted the peripheral arc to a lower AP level in sham rats. Consequently, AP at the operating point was maintained by increased SNA. Using the same experimental setup, Kamiya et al. (19) first demonstrated the HUT-induced upward neural arc shift in rabbits, although the mechanism underlying this phenomenon remained unclear. In the present study, the HUT-induced upward shift of the neural arc was completely abolished in the VL rats, indicating that the vestibular system is responsible for this shift. In fact, a lateral and pitch-direction tilt or the linear acceleration stimulates the otolith organ and alters vestibular nucleus activity (3, 29), which might alter SNA through the vestibulo-sympathetic reflex (2, 11, 17, 23, 30, 32, 40). Projection to the nucleus tractus solitarius and then the rostral ventrolateral medulla may be responsible for this sympathoexcitation (4, 34, 45). Functional convergence from the vestibular and baroreceptor afferents to the same nuclei in the nucleus tractus solitarius and the rostral ventrolateral medulla further suggests that this is the central point of interaction between the vestibular system and the baroreflex (7, 45).

Postural change from prone to HUT induces a downward fluid shift and reduces the effective circulating blood volume, reducing venous return, cardiac output, and AP (43). The reduced circulating blood volume shifts the peripheral arc to a lower AP level (35). To minimize these effects, it is important to increase the venous tone and then reduce venous compliance (12). This might be achieved by a vestibular-mediated increase in SNA, which innervates the vein. The lower shift of the peripheral arc was smaller in the sham rats than in the VL rats, suggesting that lower body blood pooling in the sham rats was less than that in the VL rats. However, Yavorcik et al. (46) found no difference in lower limb blood pooling during HUT

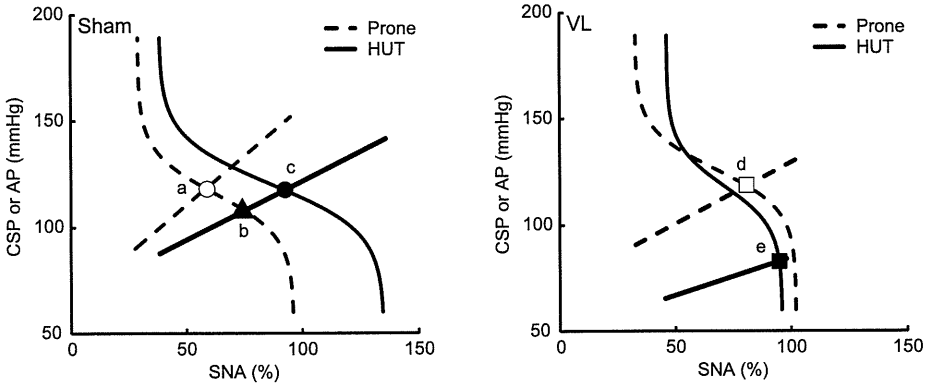

Fig. 6. Baroreflex equilibrium diagram constructed using the fitted logistic function for the neural arc and the regression line for the peripheral arc in vestibular-intact (sham) (*left*) and VL (*right*) rats. The intersection of the open circle (a) indicates the operating point of the prone position, and the solid circle (c) indicates the operating point of the HUT position in the sham rats. The intersection of the solid triangle (b) indicates the operating point without a HUT-induced neural arc shift in the sham rats. The intersection of the open square (d) shows the operating point of the prone position, and the solid square (e) shows the operating point of the HUT position in the VL rats.

in conscious cats with intact and denervated vestibular systems. We only examined renal SNA, so it is unclear from the present study whether SNAs that innervate other organs or vasculatures are increased by HUT. Kerman et al. (23) examined the responses of the renal, superior mesenteric, lumber colonic, hypogastric, and external carotid nerves to electrical stimulation of the vestibular afferent and found that renal SNA is the most sensitive response, although the other four SNAs also respond to vestibular afferent stimulation. Therefore, it is possible that HUT induced vestibular-mediated mesenteric venous vasoconstriction, and that blood pooling in the abdominal organs was less, or more blood was impelled from the abdominal organs in the sham rats than in the VL rats. This possibility should be investigated in future studies.

Interestingly, hemorrhage-induced volume depletion alone shifted the peripheral arc to a lower AP level without affecting the neural arc (35), whereas HUT shifted both the neural arc and the peripheral arc. This difference might be attributable to the existence of vestibular input, because tilt, but not hemorrhage, stimulates the vestibular organ. In this regard, the equilibrium diagram for the VL rats is similar to that drawn from the hemorrhage experiment by Sato et al. (35). The role of the vestibular system during HUT can be understood by considering the equilibrium diagrams. If the vestibular system does not operate, HUT will induce a large reduction in AP (from *point d* to *e*, Fig. 6). However, this large reduction is buffered by the vestibular system (i.e., AP was increased to *point b* by the upward shift of the peripheral arc, and was further increased to *point c* by the rightward shift of the neural arc).

The neural arc and the peripheral arc are serially connected, and the total baroreflex functional curve can be determined (21). In the VL rats, the total baroreflex functional curve was shifted downward, with a reduced maximum gain. This is consistent with the previous reports by Hosomi et al. (15, 16), in which blood loss, itself, reduced the open-loop gain of the arterial baroreflex. However, we show that, if the vestibular system is operating, the total baroreflex functional curve is restored, with an increased maximum gain. Therefore, during HUT, the vestibular system plays a significant role in maintaining the normal baroreflex functional curve, and the vestibular system and the baroreflex cooperate to maintain AP.

In conclusion, both the baroreflex and the vestibular system cooperate to maintain AP during postural changes. The vestibular system shifts the neural arc to a higher SNA level and the peripheral arc to a higher AP level and then maintains the total baroreflex functional curve. Alternatively, the total baroreflex functional curve shifts to a lower AP level, with a reduction in the maximum gain.

GRANTS

This study was supported by the Ground-Based Research Program for Space Utilization of the Japan Space Forum, a Grant-in-Aid for Scientific Research from the Japan Society for the Promotion of Science, and the Salt Science Research Foundation.

DISCLOSURES

No conflicts of interest, financial or otherwise, are declared by the author(s).

AUTHOR CONTRIBUTIONS

Author contributions: C.A. and H.M. conception and design of research; C.A., T.K., M.S., and H.M. performed experiments; C.A. and T.K. analyzed data; C.A. interpreted results of experiments; C.A. prepared figures; C.A. drafted manuscript; C.A. and H.M. edited and revised manuscript; C.A., T.K., M.S., and H.M. approved final version of manuscript.

REFERENCES

1. **Abe C, Tanaka K, Awazu C, Chen H, Morita H.** Plastic alteration of vestibulo-cardiovascular reflex induced by 2 weeks of 3-G load in conscious rats. *Exp Brain Res* 181: 639–646, 2007.
2. **Abe C, Tanaka K, Awazu C, Morita H.** Impairment of vestibular-mediated cardiovascular response and motor coordination in rats born and reared under hypergravity. *Am J Physiol Regul Integr Comp Physiol* 295: R173–R180, 2008.
3. **Amano T, Akbar M, Matsubayashi H, Sasa M.** Inhibitory effects of tandospirone, a 5-HT1A agonist, on medial vestibular nucleus neurons responding to lateral roll tilt stimulation in rats. *Brain Res* 910: 195–198, 2001.
4. **Balaban CD, Beryozkin G.** Vestibular nucleus projections to nucleus tractus solitarius and the dorsal motor nucleus of the vagus nerve: potential substrates for vestibulo-autonomic interactions. *Exp Brain Res* 98: 200–212, 1994.
5. **Casto R, Nguyen T, Printz MP.** Characterization of cardiovascular and behavioral responses to alerting stimuli in rats. *Am J Physiol Regul Integr Comp Physiol* 256: R1121–R1126, 1989.
6. **Dampney RA, Stella A, Golin R, Zanchetti A.** Vagal and sinoaortic reflexes in postural control of circulation and renin release. *Am J Physiol Heart Circ Physiol* 237: H146–H152, 1979.
7. **Destefino VJ, Reighard DA, Sugiyama Y, Suzuki T, Cotter LA, Larson MG, Gandhi NJ, Barman SM, Yates BJ.** Responses of neurons in the rostral ventrolateral medulla to whole body rotations: comparisons in decerebrate and conscious cats. *J Appl Physiol* 110: 1699–1707, 2011.
8. **Doba N, Reis DJ.** Role of the cerebellum and the vestibular apparatus in regulation of orthostatic reflexes in the cat. *Circ Res* 40: 9–18, 1974.
9. **Fessel J, Robertson D.** Orthostatic hypertension: when pressor reflexes overcompensate. *Nat Clin Pract Nephrol* 2: 424–431, 2006.
10. **Fu Q, Witkowski S, Okazaki K, Levine BD.** Effects of gender and hypovolemia on sympathetic neural responses to orthostatic stress. *Am J Physiol Regul Integr Comp Physiol* 289: R109–R116, 2005.
11. **Gotoh TM, Fujiki N, Matsuda T, Gao S, Morita H.** Roles of baroreflex and vestibulosympathetic reflex in controlling arterial blood pressure during gravitational stress in conscious rats. *Am J Physiol Regul Integr Comp Physiol* 286: R25–R30, 2004.
12. **Guyton AC, Hall JE.** *Textbook of Medical Physiology*. Amsterdam: Elsevier Saunders, 2006, p. 224.
13. **Hoffman WE, Phillips MI, Wilson E, Schmid PG.** A pressor response associated with drinking in rats. *Proc Soc Exp Biol Med* 154: 121–124, 1977.
14. **Horn KM, DeWitt JR, Nielson HC.** Behavioral assessment of sodium arsanilate induced vestibular dysfunction in rats. *Physiol Psychol* 9: 371–378, 1981.
15. **Hosomi H.** Overall characteristics of arterial pressure control system studied by mild hemorrhage. *Am J Physiol Regul Integr Comp Physiol* 234: R104–R109, 1978.
16. **Hosomi H, Baba M, Morita H.** Time-dependent changes in open-loop gains of baroreflex systems after massive hemorrhage. *Jpn J Physiol* 31: 705–715, 1981.
17. **Jian BJ, Cotter LA, Emanuel BA, Cass SP, Yates BJ.** Effects of bilateral vestibular lesions on orthostatic tolerance in awake cats. *J Appl Physiol* 86: 1552–1560, 1999.
18. **Kamiya A, Kawada T, Shimizu S, Iwase S, Sugimachi M, Mano T.** Slow head-up tilt causes lower activation of muscle sympathetic nerve activity: loading speed dependence of orthostatic sympathetic activation in humans. *Am J Physiol Heart Circ Physiol* 297: H53–H58, 2009.
19. **Kamiya A, Kawada T, Yamamoto K, Michikami D, Ariumi H, Uemura K, Zheng C, Shimizu S, Aiba T, Miyamoto T, Sugimachi M, Sunagawa K.** Resetting of the arterial baroreflex increases orthostatic sympathetic activation and prevents postural hypotension in rabbits. *J Physiol* 566: 237–246, 2005.
20. **Kawada T, Kamiya A, Li M, Shimizu S, Uemura K, Yamamoto H, Sugimachi M.** High levels of circulating angiotensin II shift the open-loop baroreflex control of splanchnic sympathetic nerve activity, heart rate and arterial pressure in anesthetized rats. *J Physiol Sci* 59: 447–455, 2009.
21. **Kawada T, Shishido T, Inagaki M, Zheng C, Yanagiya Y, Uemura K, Sugimachi M, Sunagawa K.** Estimation of baroreflex gain using a baroreflex equilibrium diagram. *Jpn J Physiol* 52: 21–29, 2002.

22. **Kent BB, Drane JW, Blumenstein B, Manning JW.** A mathematical model to assess changes in the baroreceptor reflex. *Cardiology* 57: 295–310, 1972.
23. **Kerman IA, McAllen RM, Yates BJ.** Patterning of sympathetic nerve activity in response to vestibular stimulation. *Brain Res Bull* 53: 11–16, 2000.
24. **Kerman IA, Yates BJ.** Patterning of somatosympathetic reflexes. *Am J Physiol Regul Integr Comp Physiol* 277: R716–R724, 1999.
25. **Ketch T, Biaggioni I, Robertson R, Robertson D.** Four faces of baroreflex failure: hypertensive crisis, volatile hypertension, orthostatic tachycardia, and malignant vagotonia. *Circulation* 105: 2518–2523, 2002.
26. **Krediet CT, de Bruin IG, Ganzeboom KS, Linzer M, van Lieshout JJ, Wieling W.** Leg crossing, muscle tensing, squatting, and the crash position are effective against vasovagal reactions solely through increases in cardiac output. *J Appl Physiol* 99: 1697–1703, 2005.
27. **Li J, Potts JT, Mitchell JH.** Effect of barodenervation on c-Fos expression in the medulla induced by static muscle contraction in cats. *Am J Physiol Heart Circ Physiol* 274: H901–H908, 1998.
28. **Mifflin SW, Felder RB.** Synaptic mechanisms regulating cardiovascular afferent inputs to solitary tract nucleus. *Am J Physiol Heart Circ Physiol* 259: H653–H661, 1990.
29. **Miller DM, Cotter LA, Gandhi NJ, Schor RH, Cass SP, Huff NO, Raj SG, Shulman JA, Yates BJ.** Responses of caudal vestibular nucleus neurons of conscious cats to rotations in vertical planes, before and after a bilateral vestibular neurectomy. *Exp Brain Res* 188: 175–186, 2008.
30. **Mori RL, Cotter LA, Arendt HE, Olsheski CJ, Yates BJ.** Effects of bilateral vestibular nucleus lesions on cardiovascular regulation in conscious cats. *J Appl Physiol* 98: 526–533, 2005.
31. **Muenter Swift N, Charkoudian N, Dotson RM, Suarez GA, Low PA.** Baroreflex control of muscle sympathetic nerve activity in postural orthostatic tachycardia syndrome. *Am J Physiol Heart Circ Physiol* 289: H1226–H1233, 2005.
32. **Nakamura Y, Matsuo S, Hosogai M, Kawai Y.** Vestibular control of arterial blood pressure during head-down postural change in anesthetized rabbits. *Exp Brain Res* 194: 563–570, 2009.
33. **Ray CA.** Interaction of the vestibular system and baroreflexes on sympathetic nerve activity in humans. *Am J Physiol Heart Circ Physiol* 279: H2399–H2404, 2000.
34. **Ruggiero DA, Mtui EP, Otake K, Anwar M.** Vestibular afferents to the dorsal vagal complex: substrate for vestibular-autonomic interactions in the rat. *Brain Res* 743: 294–302, 1996.
35. **Sato T, Kawada T, Inagaki M, Shishido T, Takaki H, Sugimachi M, Sunagawa K.** New analytic framework for understanding sympathetic baroreflex control of arterial pressure. *Am J Physiol Heart Circ Physiol* 276: H2251–H2261, 1999.
36. **Sato T, Kawada T, Miyano H, Shishido T, Inagaki M, Yoshimura R, Tatewaki T, Sugimachi M, Alexander J Jr, Sunagawa K.** New simple methods for isolating baroreceptor regions of carotid sinus and aortic depressor nerves in rats. *Am J Physiol Heart Circ Physiol* 276: H326–H332, 1999.
37. **Sato T, Kawada T, Sugimachi M, Sunagawa K.** Bionic technology revitalizes native baroreflex function in rats with baroreflex failure. *Circulation* 106: 730–734, 2002.
38. **Shoukas AA, Callahan CA, Lash JM, Haase EB.** New technique to completely isolate carotid sinus baroreceptor regions in rats. *Am J Physiol Heart Circ Physiol* 260: H300–H303, 1991.
39. **Tanaka K, Abe C, Awazu C, Morita H.** Vestibular system plays a significant role in arterial pressure control during head-up tilt in young subjects. *Auton Neurosci* 148: 90–96, 2009.
40. **Tanaka K, Gotoh TM, Awazu C, Morita H.** Roles of the vestibular system in controlling arterial pressure in conscious rats during a short period of microgravity. *Neurosci Lett* 397: 40–43, 2006.
41. **Tavares RF, Peres-Polon VL, Correa FM.** Mechanisms involved in the water intake-related pressor response in the rat. *J Hypertens* 20: 295–302, 2002.
42. **Waki H, Katahira K, Yamasaki M, Katsuda S, Shimizu T, Maeda M.** Cardiovascular regulation during upright standing behavior in conscious rats. *Neurosci Lett* 449: 10–14, 2009.
43. **Watenpaugh DE, Hargens AR.** The cardiovascular system in microgravity. In: *Handbook of Physiology. Environmental Physiology.* Bethesda, MD: Am. Physiol. Soc., 1996, sect. 4, vol. I, chapt. 29, p. 631–674.
44. **Yamamoto K, Kawada T, Kamiya A, Takaki H, Miyamoto T, Sugimachi M, Sunagawa K.** Muscle mechanoreflex induces the pressor response by resetting the arterial baroreflex neural arc. *Am J Physiol Heart Circ Physiol* 286: H1382–H1388, 2004.
45. **Yates BJ, Grelot L, Kerman IA, Balaban CD, Jakus J, Miller AD.** Organization of vestibular inputs to nucleus tractus solitarius and adjacent structures in cat brain stem. *Am J Physiol Regul Integr Comp Physiol* 267: R974–R983, 1994.
46. **Yavorcik KJ, Reighard DA, Misra SP, Cotter LA, Cass SP, Wilson TD, Yates BJ.** Effects of postural changes and removal of vestibular inputs on blood flow to and from the hindlimb of conscious felines. *Am J Physiol Regul Integr Comp Physiol* 297: R1777–R1784, 2009.

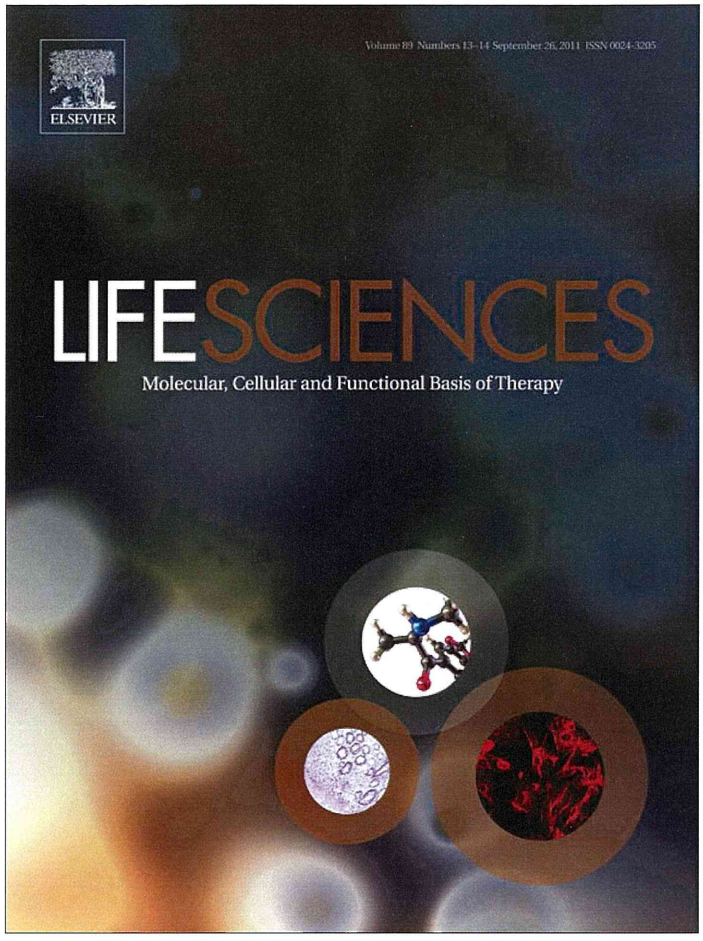

Life Sciences 89 (2011) 498–503

Contents lists available at ScienceDirect

Life Sciences

journal homepage: www.elsevier.com/locate/lifescie

Contrasting effects of moderate vagal stimulation on heart rate and carotid sinus baroreflex-mediated sympathetic arterial pressure regulation in rats

Toru Kawada [a,*], Shuji Shimizu [a], Meihua Li [a], Atsunori Kamiya [a], Kazunori Uemura [a], Yusuke Sata [a], Hiromi Yamamoto [b], Masaru Sugimachi [a]

[a] Department of Cardiovascular Dynamics, National Cerebral and Cardiovascular Center Research Institute, Osaka 565-8565, Japan
[b] Division of Cardiology, Department of Internal Medicine, Kinki University School of Medicine, Osaka 589-8511, Japan

ARTICLE INFO

Article history:
Received 30 March 2011
Accepted 19 July 2011

Keywords:
Carotid sinus baroreflex
Open-loop analysis
Sympathetic nerve activity

ABSTRACT

Aims: To examine whether moderate efferent vagal nerve stimulation (VNS) attenuates the carotid sinus baroreflex-mediated arterial pressure (AP) regulation via its antagonism to the sympathetic system.
Main methods: Carotid sinus baroreceptor regions were isolated from the systemic circulation in eight anesthetized and vagotomized rats. A staircase-wise input was imposed on carotid sinus pressure (CSP) with or without efferent VNS (20 Hz, 2 ms, 1–4 V), while the responses in AP, heart rate (HR), and splanchnic sympathetic nerve activity (SNA) were measured.
Key findings: A multiple linear regression analysis indicated that VNS decreased the minimum HR in the CSP–HR relationship by 58.2 ± 4.9 beats/min ($P<0.01$) from its reference value of 387.0 ± 5.8 beats/min. Although VNS significantly decreased an intercept of the SNA–AP relationship, it did not affect parameters of the CSP–AP relationship or the CSP–SNA relationship significantly. The operating-point AP of the baroreflex was decreased by 2.8 ± 1.0 mm Hg ($P<0.01$) during VNS, which was less than 3% of the reference value of 117.7 ± 1.2 mm Hg.
Significance: VNS, at an intensity of decreasing HR by approximately 13%, does not acutely attenuate the baroreflex-mediated sympathetic AP regulation.

Introduction

Vagal nerve stimulation (VNS) has been proposed as a new therapeutic approach to improve long-term survival of chronic heart failure in rats (Li et al., 2004). The feasibility of VNS in chronic heart failure patients has been reported (De Ferrari et al., 2011; Schwartz, 2010). Because excess sympathetic activity has deleterious effects on the failing heart, VNS is considered to provide beneficial effects through its antagonism to the sympathetic system. On the other hand, if VNS significantly attenuates the sympathetic arterial pressure (AP) regulation through the antagonism to the sympathetic system, resulting adverse effects such as reduced orthostatic tolerance may limit the utility of VNS. In fact, VNS can cause bradycardia and hypotension depending on the intensity of stimulation (Shimizu et al., 2009). The effect of VNS on the sympathetic AP regulation, however, is not fully understood, partially because the arterial baroreflex always buffers changes in AP and obscures the pure VNS effect on AP. Another concern is that the magnitude of VNS-induced antagonism to the sympathetic system could vary depending on the level of sympathetic nerve activity (SNA). To elucidate the pure effect of VNS on the sympathetic AP regulation at various levels of SNA, a baroreflex open-loop analysis described below is required.

The sympathetic arterial baroreflex can be divided into two principal subsystems: a neural arc subsystem from pressure input to efferent SNA, and a peripheral arc subsystem from SNA to AP (Mohrman and Heller, 2006; Ikeda et al., 1996; Sato et al., 1999a, 1999b). Under normal physiological conditions, AP affects SNA through the neural arc, while SNA in turn affects AP through the peripheral arc. This closed-loop operation makes it difficult to identify the input–output relationships of the two arcs separately (Kawada et al., 1997; Kamiya et al., 2011). To circumvent the problem, a baroreflex open-loop analysis using an isolated carotid sinus preparation has been employed (Kawada et al., 2009, 2010). In the present study, a hypothesis that moderate efferent VNS attenuates the baroreflex-mediated sympathetic AP regulation was tested in anesthetized and vagotomized rats.

Materials and methods

Surgical preparation

Animal care was provided in strict accordance with the *Guiding Principles for the Care and Use of Animals in the Field of Physiological Sciences*, approved by the Physiological Society of Japan. All protocols were reviewed and approved by the Animal Subject Committee of National Cerebral and Cardiovascular Center. Eight male Sprague–

* Corresponding author at: Department of Cardiovascular Dynamics, National Cerebral and Cardiovascular Center Research Institute, 5-7-1 Fujishirodai, Suita, Osaka 565-8565, Japan. Tel.: +81 6 6833 5012x2427; fax: +81 6 6835 5403.
E-mail address: torukawa@res.ncvc.go.jp (T. Kawada).

0024-3205/$ – see front matter © 2011 Elsevier Inc. All rights reserved.
doi:10.1016/j.lfs.2011.07.026

Dawley rats (408–590 g) were anesthetized by an intraperitoneal injection (2 ml/kg) of a mixture of α-chloralose (40 mg/ml) and urethane (250 mg/ml), and ventilated mechanically with oxygen-supplied room air. The depth of anesthesia was maintained with a 20-fold diluted solution of the above anesthetic mixture infused from the right femoral vein (2–3 ml kg^{-1} h^{-1}). Another venous catheter was inserted into the left femoral vein to supply Ringer solution (6 ml kg^{-1} h^{-1}). AP was measured from a catheter inserted into the right femoral artery. Heart rate (HR) was detected from AP using a cardiotachometer (AT-601G, Nihon Kohden, Tokyo, Japan). Body temperature of the animal was maintained by a heating pad at approximately 38 °C.

A postganglionic branch of the splanchnic sympathetic nerve was exposed through a left flank incision. A pair of stainless steel wire electrodes (Bioflex wire, AS633, Cooner Wire, CA, USA) was attached to the nerve to record SNA. The nerve and electrodes were secured and insulated with silicone glue (Kwik-Sil, World Precision Instruments, FL, USA). To quantify SNA, a preamplified nerve signal was band-pass filtered at 150–1000 Hz, and then full-wave rectified and low-pass filtered with a cut-off frequency of 30 Hz using analog circuits. Pancuronium bromide (0.4 mg kg^{-1} h^{-1}) was given continuously to prevent muscular activity from contaminating SNA. At the end of the experiment, a bolus injection of a ganglionic blocker hexamethonium bromide (60 mg/kg) was given to confirm the disappearance of SNA and to measure the noise level.

Carotid sinus baroreceptor regions were isolated from the systemic circulation according to previously reported procedures (Shoukas et al., 1991; Sato et al., 1999a, 1999b) with modifications. Briefly, a 7–0 polypropylene suture with a fine needle (PROLENE, Ethicon, GA, USA) was passed through the tissue between the external and internal carotid arteries, and the external carotid artery was ligated close to the carotid bifurcation. The internal carotid artery was embolized with two to three steel balls (0.8 mm in diameter, Tsubaki Nakashima, Nara, Japan) injected from the common carotid artery. The isolated carotid sinuses were filled with Ringer solution through catheters inserted into the common carotid arteries. Carotid sinus pressure (CSP) was controlled using a servo-controlled piston pump. Heparin sodium (100 U/kg) was given intravenously to prevent blood coagulation.

Bilateral vagal and aortic depressor nerves were sectioned at the neck to avoid reflexes from the cardiopulmonary region and aortic arch. A pair of stainless steel wire electrodes (Bioflex wire, AS633, Cooner Wire, CA, USA) was attached to the sectioned right vagus for efferent VNS. The nerve and electrodes were secured and insulated with silicone glue (Kwik-Sil, World Precision Instruments, FL, USA).

Protocol

After the surgical procedures were completed, responses in SNA, AP, and HR to a CSP input were monitored for more than 30 min. The rat was excluded from the study if the reflex responses became smaller within this stabilization period. Possible causes for the deterioration of the baroreflex responses include surgical damage to the carotid sinus nerves and brain ischemia due to bilateral carotid occlusion. After the stabilization period, CSP was matched to instantaneous AP to make the carotid sinus baroreflex virtually closed, and baseline hemodynamic data were recorded for 10 min.

To estimate open-loop static input–output relationship of the carotid sinus baroreflex, CSP was first decreased to 60 mm Hg for 4 min. CSP was then increased from 60 to 180 mm Hg every minute in increments of 20 mm Hg (Kawada et al., 2009, 2010). The staircase-wise input cycle was repeated throughout the protocol. VNS was applied to the right vagus at 20 Hz with a pulse duration of 2 ms. The square pulse with this pulse duration was not intended to mimic naturally occurring vagal nerve activity; rather, the stimulation parameters were determined based on a previous study showing that VNS with this setting can produce significant bradycardia (Mizuno et al., 2011). The amplitude of VNS was adjusted (1–4 V) in each animal to reduce HR by approximately 50 beats/min before starting the staircase-wise input protocol. Data were recorded for two cycles before VNS, three cycles during VNS, and two cycles after VNS.

Data analysis

Data were sampled at 200 Hz using a 16-bit analog-to-digital converter and stored on a dedicated laboratory computer system. There was a transient response after changing the level of CSP. To estimate the input–output relationship at the steady state, mean AP, HR, and SNA were calculated during the last 10 s at each CSP level of the staircase-wise input. In each rat, the noise level of SNA measured after the administration of hexamethonium bromide was defined as zero. Because the absolute amplitude of SNA varied among animals depending on the recording conditions, mean SNA measured at the CSP level of 60 mm Hg in the first cycle was defined as 100 au (arbitrary units).

Static characteristics of the carotid sinus total-loop baroreflex (CSP–AP relationship), HR control (CSP–HR relationship), and neural arc (CSP–SNA relationship) approximated an inverse sigmoid curve, and were quantified using a four-parameter logistic function as follows (Kent et al., 1972):

$$y = \frac{P_1}{1 + \exp[P_2(\mathrm{CSP} - P_3)]} + P_4$$

where y denotes the output value (AP, HR, or SNA); P_1 is the response range of y; P_2 is the slope coefficient; P_3 is the midpoint of the sigmoid curve on the CSP axis; and P_4 is the minimum value of y. Although the slope of an inverse sigmoid curve is negative, for convenience sake, the maximum gain or slope of the logistic function (G_{max}) was calculated as a positive value of $P_1P_2/4$.

Static characteristics of the peripheral arc (SNA–AP relationship) approximated a straight line, and were quantified using a linear regression as follows:

$$\mathrm{AP} = a \times \mathrm{SNA} + b$$

where a and b represent the slope and intercept, respectively.

Statistical analysis

All data are presented as mean and SE values. Changes in each parameter obtained from 7 staircase-wise input cycles of 8 animals (56 values) were analyzed together by a multiple linear regression as follows (Glantz and Slinker, 2001):

$$p = C + B_{\mathrm{Time}} \times N + B_{\mathrm{VNS}} \times D_{\mathrm{VNS}} + B_1 \times D_1 + B_2 \times D_2 + \cdots + B_{k-1} \times D_{k-1}$$

where p is the parameter value; C is a constant term of the multiple linear regression; B_{Time} is a coefficient for the time effect; N is a cycle number ranging 0 (the first cycle) through 6 (the last cycle); B_{VNS} is a coefficient for the VNS effect; D_{VNS} is a dummy variable encoding VNS ($D_{\mathrm{VNS}} = 0$: no stimulation, $D_{\mathrm{VNS}} = 1$: during stimulation); D_1 through D_{k-1} are dummy variables encoding k different animals (see Table 1); and B_1 through B_{k-1} are coefficients for inter-individual variations. In the present study, because the time effect and VNS effect are of major concern, B_{Time} and B_{VNS} alone are reported together with C. Note that C predicts the parameter value in the first cycle ($N = 0$ and $D_{\mathrm{VNS}} = 0$) and serves as a reference value to interpret the magnitudes of the time effect and VNS effect. B_{Time} and B_{VNS} were tested whether they were significantly different from zero, with a significance level set at $P<0.05$ (Glantz and Slinker, 2001).

Table 1
Dummy variables encoding eight different animals.

	D_1	D_2	D_3	D_4	D_5	D_6	D_7
Animal 1	1	0	0	0	0	0	0
Animal 2	0	1	0	0	0	0	0
Animal 3	0	0	1	0	0	0	0
Animal 4	0	0	0	1	0	0	0
Animal 5	0	0	0	0	1	0	0
Animal 6	0	0	0	0	0	1	0
Animal 7	0	0	0	0	0	0	1
Animal 8	−1	−1	−1	−1	−1	−1	−1

To encode 8 different animals, only 7 different dummy variables are needed. An effect coding was used to model the inter-individual differences in a multiple linear regression analysis (Glantz and Slinker, 2001).

Results

Before starting the staircase-wise input protocol, CSP was matched to instantaneous AP through a servo control. Mean AP and HR under the carotid sinus baroreflex closed-loop conditions were 114.6 ± 5.3 mm Hg and 435.9 ± 11.7 beats/min, respectively. After the staircase-wise input protocol, hexamethonium bromide was administered, which decreased mean AP and HR to 54.0 ± 4.4 mm Hg and 350.9 ± 12.7 beats/min, respectively.

The left panels of Fig. 1 shows typical recordings of CSP, AP, HR, and SNA before, during, and after VNS in one animal. A white line in the SNA recording represents a 2-s moving averaged signal. The staircase-wise elevation in CSP decreased AP, HR, and SNA. VNS, applied at the 21st minute, immediately decreased HR, and thereafter HR remained decreased until the end of VNS at the 51st minute. The cessation of VNS returned HR toward the pre-stimulation level. VNS did not appear to affect the AP or SNA response. In the right panels of Fig. 1, the administration of hexamethonium bromide diminished SNA, which was followed by decreases in AP and HR.

The open-loop static characteristics of the carotid sinus total-loop baroreflex showed an inverse sigmoidal relationship regardless of VNS (Fig. 2, the top row). A multiple linear regression analysis on parameters of the total-loop baroreflex indicated that P_3 slightly decreased with time (0.8 mm Hg per cycle) (Table 2). Other parameters did not show a significant time effect. None of the parameters of the total-loop baroreflex showed a significant VNS effect.

The HR control also revealed an inverse sigmoidal relationship between CSP and HR regardless of VNS (Fig. 2, the second row). Although P_1 slightly decreased with time (1.7 beats/min per cycle), other parameters did not show a significant time effect (Table 2). VNS significantly decreased P_4 by 58.2 beats/min, and also decreased P_3 by 4.2 mm Hg. There was no significant VNS effect on P_1, P_2, or G_{max}.

The neural arc of the carotid sinus baroreflex showed an inverse sigmoidal relationship regardless of VNS (Fig. 2, the third row). The parameters of the neural arc except P_1 and G_{max} showed a significant time effect to some degree (Table 2). None of the parameters of the neural arc revealed a significant VNS effect.

The peripheral arc of the carotid sinus baroreflex approximated a straight line regardless of VNS (Fig. 2, the fourth row). There was no significant time effect on the slope or intercept of the peripheral arc (Table 2). VNS did not affect the slope, but significantly decreased the intercept by 5.8 mm Hg.

When the neural arc and the peripheral arc are drawn on a pressure–SNA plane, the intersection provides an operating point of the carotid sinus baroreflex (Fig. 2, the bottom row). While the operating-point AP did not change with time, the operating-point SNA increased slightly with time (1.3 au per cycle) (Table 2). VNS reduced the operating-point AP by 2.8 mm Hg without a significant effect on the operating-point SNA.

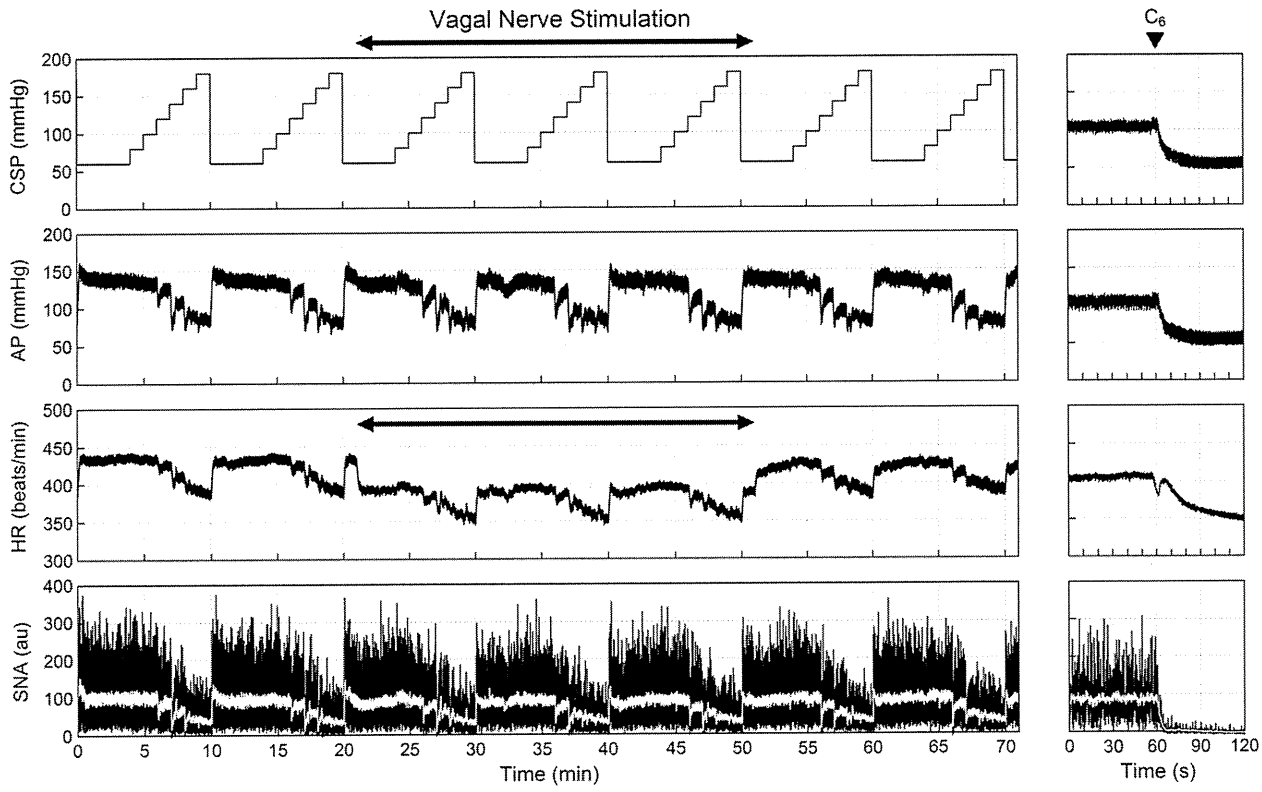

Fig. 1. Typical experimental recordings of carotid sinus pressure (CSP), arterial pressure (AP), heart rate (HR), and sympathetic nerve activity (SNA). A staircase-wise CSP input was repeated before, during, and after vagal nerve stimulation. The white line in the SNA recoding indicates a 2-s moving-averaged signal. The horizontal arrows indicate the duration of the vagal nerve stimulation. The right panels show the recordings of the intravenous bolus injection of hexamethonium bromide (C_6).

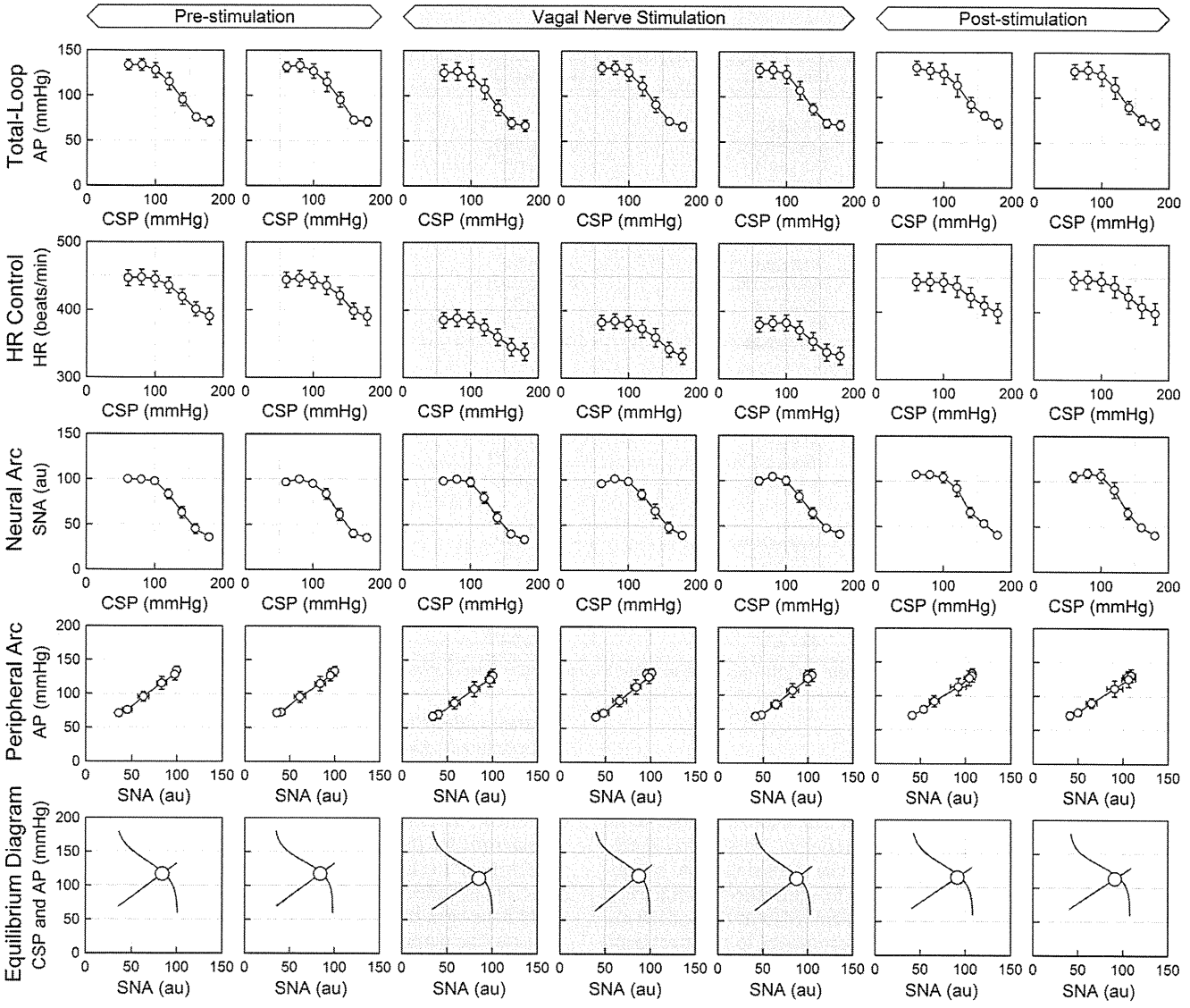

Fig. 2. The open-loop static characteristics of the carotid sinus total-loop baroreflex (top row), heart rate (HR) control (second row), neural arc (third row), peripheral arc (fourth row), and the baroreflex equilibrium diagram (bottom row). CSP: carotid sinus pressure, AP: arterial pressure, SNA: sympathetic nerve activity. The characteristics of the carotid sinus total-loop baroreflex, HR control, and neural arc approximated an inverse sigmoid curve. The characteristics of the peripheral arc approximated a straight line. The baroreflex equilibrium diagram was obtained by plotting the neural arc and peripheral arc on a pressure–SNA plane. The intersection of the two arcs (an open circle) indicates the operating point of the carotid sinus baroreflex.

Discussion

Interactions between the vagal and sympathetic systems

The efferent vagal nerve controls the heart via direct and indirect mechanisms (Kitamura et al., 2000; Mizuno et al., 2007). In the indirect mechanism, the vagal nerve antagonizes the sympathetic nerve at pre- and post-synaptic sites (Muscholl, 1980; Irisawa et al., 1993), producing significant vago-sympathetic interactions in controlling HR (Levy, 1971; Kawada et al., 1996). Although VNS reduces left ventricular contractility mainly via its negative chronotropic effect (Matsuura et al., 1997), it can also reduce the contractility via the antagonism to background sympathetic tone (Nakayama et al., 2001). These lines of evidence suggest that VNS would attenuate the sympathetic AP regulation depending on the level of SNA.

Contrary to our presumption, VNS, at an intensity of reducing HR by approximately 58 beats/min (13% of a closed-loop baseline HR), did not affect the carotid sinus total-loop baroreflex characteristics. The slope of the peripheral arc was not changed significantly during VNS, suggesting a preserved sympathetic AP regulation. On the other hand, the intercept of the peripheral arc was decreased significantly during VNS. The intercept, however, is estimated by a linear extrapolation of the SNA–AP relationship toward zero SNA. Because actually measured AP after ganglionic blockade was approximately 54 mm Hg and higher than the intercept, there should exist nonlinearity in the SNA–AP relationship as SNA approaches zero.

To assess the VNS effect within a linear range of the peripheral arc, the neural arc and peripheral arc were drawn on a single pressure–SNA plane (Fig. 2, the bottom row). The operating-point AP was decreased by 2.8 mm Hg during VNS, which was less than 3% of the reference value of 117 mm Hg (Table 2). Therefore, despite possible vago-sympathetic interactions in controlling HR (Levy, 1971; Kawada et al., 1996) and ventricular contractility (Nakayama et al., 2001), VNS may not acutely interfere with the carotid sinus baroreflex-mediated sympathetic AP regulation.

Table 2
Effects of time and vagal nerve stimulation (VNS) on parameters of the total baroreflex, heart rate (HR) control, neural arc, and peripheral arc.

	Constant (C)	Time effect (B_{Time})	VNS effect (B_{VNS})	R^2
Total baroreflex				
P_1, mm Hg	66.4 ± 2.5	−0.6 ± 0.5	0.2 ± 2.1	0.87
P_2, mm Hg^{-1}	0.085 ± 0.006	0.002 ± 0.001	0.001 ± 0.005	0.37
P_3, mm Hg	132.3 ± 1.4	−0.8 ± 0.3**	−1.5 ± 1.2	0.93
P_4, mm Hg	68.0 ± 2.1	0.3 ± 0.4	−3.0 ± 1.7	0.85
G_{max}, mm Hg/mm Hg	1.46 ± 0.07	0.01 ± 0.02	0.01 ± 0.06	0.89
HR control				
P_1, beats/min	61.6 ± 3.1	−1.7 ± 0.6*	−3.9 ± 2.6	0.76
P_2, mm Hg^{-1}	0.082 ± 0.006	0.001 ± 0.001	0.010 ± 0.006	0.54
P_3, mm Hg	138.2 ± 1.6	−0.3 ± 0.3	−4.2 ± 1.4**	0.90
P_4, beats/min	387.0 ± 5.8	1.6 ± 1.2	−58.2 ± 4.9**	0.87
G_{max}, beats min^{-1} mm Hg^{-1}	1.31 ± 0.08	−0.02 ± 0.02	0.02 ± 0.07	0.87
Neural arc				
P_1, au	68.6 ± 2.5	−0.5 ± 0.5	−2.6 ± 2.1	0.64
P_2, mm Hg^{-1}	0.082 ± 0.007	0.004 ± 0.001*	0.000 ± 0.006	0.46
P_3, mm Hg	135.9 ± 1.5	−1.0 ± 0.3**	−0.6 ± 1.2	0.92
P_4, au	29.6 ± 2.3	2.1 ± 0.5**	−0.6 ± 1.9	0.61
G_{max}, au/mm Hg	1.45 ± 0.13	0.05 ± 0.03	−0.09 ± 0.11	0.65
Peripheral arc				
Slope, mm Hg/au	0.98 ± 0.04	−0.01 ± 0.01	0.05 ± 0.03	0.59
Intercept, mm Hg	36.2 ± 2.4	−0.5 ± 0.5	−5.8 ± 2.0**	0.87
Operating point				
AP, mm Hg	117.7 ± 1.2	−0.5 ± 0.2	−2.8 ± 1.0**	0.94
SNA, au	82.5 ± 1.7	1.3 ± 0.4**	−1.1 ± 1.4	0.76

*$P<0.05$ and **$P<0.01$ by a multiple linear regression analysis. AP: arterial pressure, SNA: sympathetic nerve activity, au: arbitrary units.

VNS as a therapeutic approach

VNS has been shown to prevent lethal arrhythmia after acute myocardial ischemia in dogs (Vanoli et al., 1991). VNS, at an intensity of reducing HR by approximately 10%, can improve a long-term survival of chronic heart failure in rats (Li et al., 2004). Early short-term VNS also attenuates left ventricular remodeling in rabbits (Uemura et al., 2010). The antagonism to sympathetic overactivity through afferent (Kashihara et al., 2004) and efferent (Kawada et al., 2006, 2008) vagal pathways probably contribute to the treatment effects. β-Adrenergic blockade alone, however, cannot prevent the left ventricular remodeling in rats (Litwin et al., 1999), suggesting the importance of other mechanisms than β-adrenergic blockade. For instance, an anti-inflammatory effect through nicotinic receptors (Tracey, 2002; Altavilla et al., 2006) and an expression of tissue inhibitor of matrix metalloproteinase-1 through muscarinic receptors (Uemura et al., 2007) are reported.

Aside from the studies on treatment mechanisms, possible adverse effects of VNS need to be examined. Previous studies have demonstrated that the carotid sinus baroreflex function is depressed in canine heart failure (White, 1981; Wang et al., 1991). In chronic heart failure rats, the open-loop carotid sinus baroreflex function is depressed in such a way that AP becomes more labile to small pressure disturbances compared to normal rats (Kawada et al., 2010). If VNS further attenuated the sympathetic AP regulation, a serious adverse effect on the AP regulation could have followed. In the present study, whether efferent VNS affects sympathetic AP regulation was examined. The carotid sinus baroreflex-mediated sympathetic AP regulation was maintained during efferent VNS despite a significant bradycardic effect. In the case of VNS on the intact vagal nerve, activation of afferent vagal pathways may inhibit SNA. Whether afferent VNS modifies the carotid sinus baroreflex function was not examined in the present study and awaits further investigations.

Limitations

First, the effect of VNS on the carotid sinus baroreflex was examined in normal anesthetized and vagotomized rats. Because anesthesia affects the autonomic nerve activities, the results may not be directly extrapolated to the baroreflex function under conscious conditions. Second, VNS was applied continuously for 30 min and its acute effect was examined. Further studies are required to evaluate the effect of chronic VNS on the baroreflex function. Third, mechanisms for the contrasting effects of VNS on HR and AP were not clarified. It is likely that VNS, at an intensity used in the present study, did not affect venous return significantly, and a decrease in HR might have been counterbalanced by an increase in stroke volume to keep cardiac output similar regardless of VNS. Further studies are needed to verify this assumption. Fourth, increasing the intensity of VNS can reduce HR by more than 150 beats/min in rats (Mizuno et al., 2011), which may accompany significant hypotension such as that observed in rabbits (Shimizu et al., 2009). The effect of such a strong VNS on the baroreflex function is of physiological interest but beyond the scope of this study. Finally, considering the treatment use of VNS, it would be better to superimpose VNS over a native vagal tone. In the present study, however, we aimed to identify the possible effect of efferent VNS without an influence of afferent VNS using vagotomized rats. Although efferent VNS may simply replace the lost vagal tone, because vagal tone is thought to be diminished in heart failure, the present study may partly mimic the diseased conditions.

Conclusion

Although efferent VNS, at an intensity of treatment use, slightly decreased the intercept of the peripheral arc and the operating-point AP, it did not affect parameters of the carotid sinus total-loop baroreflex and the neural arc significantly, suggesting a limited ability of VNS to attenuate the sympathetic AP regulation. The present study would provide a rationale for the safety of VNS with regard to the carotid sinus baroreflex-mediated sympathetic AP regulation.

Conflict of interest statement

The authors declare that there are no conflicts of interest.

Acknowledgments

This study was supported by Health and Labour Sciences Research Grants (H19-nano-Ippan-009, H20-katsudo-Shitei-007, and H21-nano-Ippan-005) from the Ministry of Health, Labour and Welfare of Japan; the Grants-in-Aid for Scientific Research (C-23592319) promoted by the Ministry of Education, Culture, Sports, Science and Technology of Japan; and by the Industrial Technology Research Grant Program from the New Energy and Industrial Technology Development Organization (NEDO) of Japan.

References

Altavilla D, Guarini S, Bitto A, Mioni C, Giuliani D, Bigiani A, et al. Activation of the cholinergic anti-inflammatory pathway reduces NF-κB activation, blunts TNF-α production, and protects againts splanchic artery occlusion shock. Shock 2006;25: 500–6.

De Ferrari GM, Crijns HJ, Borggrefe M, Milasinovic G, Smid J, Zabel M, et al. for the CardioFit Multicenter Trial Investigators. Chronic vagus nerve stimulation: a new and promising therapeutic approach for chronic heart failure. Eur Heart J 2011;32: 847–55.

Glantz SA, Slinker BK. Primer of applied regression & analysis of variance. 2nd ed. New York: McGraw-Hill; 2001.

Ikeda Y, Kawada T, Sugimachi M, Kawaguchi O, Shishido T, Sato T, et al. Neural arc of baroreflex optimizes dynamic pressure regulation in achieving both stability and quickness. Am J Physiol 1996;271:H882–90.

Irisawa H, Brown HF, Giles W. Cardiac pacemaking in the sinoatrial node. Physiol Rev 1993;73:197–227.

Kamiya A, Kawada T, Shimizu S, Sugimachi M. Closed-loop spontaneous baroreflex transfer function is inappropriate for system identification of neural arc but partly accurate for peripheral arc: predictability analysis. J Physiol 2011;589: 1769–90.

Kashihara K, Kawada T, Li M, Sugimachi M, Sunagawa K. Bezold–Jarisch reflex blunts arterial baroreflex via the shift of neural arc toward lower sympathetic nerve activity. Jpn J Physiol 2004;54:395–404.

Kawada T, Ikeda Y, Sugimachi M, Shishido T, Kawaguchi O, Yamazaki T, et al. Bidirectional augmentation of heart rate regulation by autonomic nervous system in rabbits. Am J Physiol 1996;271:H288–95.

Kawada T, Sugimachi M, Sato T, Miyano H, Shishido T, Miyashita H, et al. Closed-loop identification of carotid sinus baroreflex open-loop transfer characteristics in rabbits. Am J Physiol 1997;273:H1024–31.

Kawada T, Yamazaki T, Akiyama T, Li M, Ariumi H, Mori H, et al. Vagal stimulation suppresses ischemia-induced myocardial interstitial norepinephrine release. Life Sci 2006;78:882–7.

Kawada T, Yamazaki T, Akiyama T, Kitagawa H, Shimizu S, Mizuno M, et al. Vagal stimulation suppresses ischemia-induced myocardial interstitial myoglobin release. Life Sci 2008;83:490–5.

Kawada T, Kamiya A, Li M, Shimizu S, Uemura K, Yamamoto H, et al. High levels of circulating angiotensin II shift the open-loop baroreflex control of splanchnic sympathetic nerve activity, heart rate and arterial pressure in anesthetized rats. J Physiol Sci 2009;59:447–55.

Kawada T, Li M, Kamiya A, Shimizu S, Uemura K, Yamamoto H, et al. Open-loop dynamic and static characteristics of the carotid sinus baroreflex in rats with chronic heart failure after myocardial infarction. J Physiol Sci 2010;60:283–98.

Kent BB, Drane JW, Blumenstein B, Manning JW. A mathematical model to assess changes in the baroreceptor reflex. Cardiology 1972;57:295–310.

Kitamura H, Yokoyama M, Akita H, Matsushita K, Kurachi Y, Yamada M. Tertiapin potently and selectively blocks muscarinic K^+ channels in rabbit cardiac myocytes. J Pharmacol Exp Ther 2000;293:196–205.

Levy MN. Sympathetic–parasympathetic interactions in the heart. Circ Res 1971;29: 437–45.

Li M, Zheng C, Sato T, Kawada T, Sugimachi M, Sunagawa K. Vagal nerve stimulation markedly improves long-term survival after chronic heart failure in rats. Circulation 2004;109:120–4.

Litwin SE, Katz SE, Morgan JP, Douglas PS. Effects of propranolol treatment on left ventricular function and intracellular calcium regulation in rats with postinfarction heart failure. Br J Pharmacol 1999;127:1671–9.

Matsuura W, Sugimachi M, Kawada T, Sato T, Shishido T, Miyano H, et al. Vagal stimulation decreases left ventricular contractility mainly through negative chronotropic effect. Am J Physiol 1997;273:H534–9.

Mizuno M, Kamiya A, Kawada T, Miyamoto T, Shimizu S, Sugimachi M. Muscarinic potassium channels augment dynamic and static heart rate responses to vagal stimulation. Am J Physiol Heart Circ Physiol 2007;293:H1564–70.

Mizuno M, Kawada T, Kamiya A, Miyamoto T, Shimizu S, Shishido T, et al. Exercise training augments the dynamic heart rate response to vagal but not sympathetic stimulation in rats. Am J Physiol Regul Integr Comp Physiol 2011;300:R969–77.

Mohrman DE, Heller LJ. Cardiovascular physiology. 6th ed. New York: McGraw Hill; 2006.

Muscholl E. Peripheral muscarinic control of norepinephrine release in the cardiovascular system. Am J Physiol 1980;239:H713–20.

Nakayama Y, Miyano H, Shishido T, Inagaki M, Kawada T, Sugimachi M, et al. Heart rate-independent vagal effect on end-systolic elastance of the canine left ventricle under various levels of sympathetic tone. Circulation 2001;104:2277–9.

Sato T, Kawada T, Inagaki M, Shishido T, Takaki H, Sugimachi M, et al. New analytic framework for understanding sympathetic baroreflex control of arterial pressure. Am J Physiol 1999a;276:H2251–61.

Sato T, Kawada T, Miyano H, Shishido T, Inagaki M, Yoshimura R, et al. New simple methods for isolating baroreceptor regions of carotid sinus and aortic depressor nerves in rats. Am J Physiol Heart Circ Physiol 1999b;276:H326–32.

Schwartz PJ. Vagal stimulation for heart diseases: from animals to men. — An example of translational cardiology. Circ J 2010;75:20–7.

Shimizu S, Akiyama T, Kawada T, Shishido T, Yamazaki T, Kamiya A, et al. In vivo direct monitoring of vagal acetylcholine release to the sinoatrial node. Auton Neurosci 2009;148:44–9.

Shoukas AA, Callahan CA, Lash JM, Haase EB. New technique to completely isolate carotid sinus baroreceptor regions in rats. Am J Physiol Heart Circ Physiol 1991;260:H300–3.

Tracey KJ. The inflammatory reflex. Nature 2002;420:853–9.

Uemura K, Li M, Tsutsumi T, Yamazaki T, Kawada T, Kamiya A, et al. Efferent vagal nerve stimulation induces tissue inhibitor of metalloproteinase-1 in myocardial ischemia–reperfusion injury in rabbit. Am J Physiol Heart Circ Physiol 2007;293: H2254–61.

Uemura K, Zheng C, Li M, Kawada T, Sugimachi M. Early short-term vagal nerve stimulation attenuates cardiac remodeling after reperfused myocardial infarction. J Card Fail 2010;16:689–99.

Vanoli E, De Ferrari GM, Stramba-Badiale M, Hull Jr SS, Foreman RD, Schwartz PJ. Vagal stimulation and prevention of sudden death in conscious dogs with a healed myocardial infarction. Circ Res 1991;68:1471–81.

Wang W, Chen JS, Zucker IH. Carotid sinus baroreceptor reflex in dogs with experimental heart failure. Circ Res 1991;68:1294–301.

White CW. Abnormalities in baroreflex control of heart rate in canine heart failure. Am J Physiol 1981;240:H793–9.